# An Extended $\beta$-Strand Mimic for a Larger Artificial $\beta$-Sheet

**James S. Nowick,* Mason Pairish, In Quen Lee, Darren L. Holmes, and Joseph W. Ziller**

*Contribution from the Department of Chemistry, University of California, Irvine, Irvine, California 92697-2025*

*Received November 5, 1996*[⊗]

**Abstract:** This paper reports the development of $\beta$-strand mimic **B**, which duplicates the hydrogen-bonding functionality of one edge of a tetrapeptide $\beta$-strand. When attached to a tripeptide by a suitable linking group, $\beta$-strand mimic **B** forms a hydrogen-bonded antiparallel $\beta$-sheet structure, artificial $\beta$-sheet **2**. $\beta$-Strand mimic **B** is based upon a 5-hydrazino-2-methoxybenzoic acid building block. The first half of the paper describes synthetic, IR and $^1$H NMR spectroscopic, X-ray crystallographic, and molecular modeling studies of 5-hydrazino-2-methoxybenzoic acid derivatives and related molecules. These studies establish that hydrazide derivatives of 5-hydrazino-2-methoxybenzoic acid adopt a conformation similar to that of a peptide $\beta$-strand and are suitable for use as $\beta$-strand mimics. The second half of the paper describes synthetic and $^1$H NMR spectroscopic studies of artificial $\beta$-sheet **2** and of controls **20** and **21**, which resemble the peptidomimetic and peptide strands of **2**. These experiments indicate that **2** adopts a conformation and hydrogen-bonding pattern similar to that of an antiparallel $\beta$-sheet and establish that $\beta$-strand mimic **B** can induce $\beta$-sheet formation in an attached peptide strand.

## Introduction

The mimicry of peptide and protein structures has emerged as a focal point of bioorganic and medicinal chemistry. This emergence has been marked by the appearance of at least 15 review articles since 1990 on different aspects of peptidomimetic chemistry.[1] As a result of the recent activity in this field, there is now a growing appreciation that peptidomimetic chemistry can serve as a basis for drug development and that peptidomimetic model systems can provide fundamental insights into the folding and structure of proteins.

Recently, compounds that mimic the conformational and hydrogen-bonding properties of peptide $\beta$-strands have begun to attract attention. In 1988, Kemp and Bowen reported that 2,8-diaminoepindolidione duplicates the hydrogen-bonding functionality of one edge of a peptide $\beta$-strand.[1a,2,3] When attached to peptide strands by suitable linking groups, this compound serves as a template to induce $\beta$-sheet formation. By measuring the relative stabilities of these $\beta$-sheets, Kemp and co-workers were able to determine the $\beta$-sheet forming propensities of different amino acids. Two years later, Martin and co-workers developed 1,2,3-trisubstituted cyclopropanes as peptide isosteres that mimic the $\beta$-strand conformation of peptides bound by proteolytic enzymes.[4] Renin and collagenase inhibitors incorporating these $\beta$-strand mimics were prepared and studied. Smith, Hirschmann, and co-workers invented 3,5-linked pyrroline-4-ones, which duplicate the main-chain conformation and side-chain placement of $\beta$-strands, and applied these compounds to the creation of peptidomimetic inhibitors of HIV protease and renin.[5] At the beginning of 1996, Michne and Schroeder reported that a 3-amino-4(*1H*)-quinoline template, which is

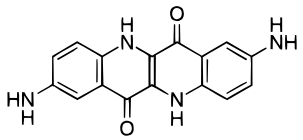

2,8-diaminoepindolidione

[⊗] Abstract published in *Advance ACS Abstracts,* May 15, 1997.

(1) Kemp, D. S. *Trends Biotechnol.* **1990**, *8*, 249. (b) Hölzemann, G. *Kontakte* **1991**, 3. (c) Hölzemann, G. *Kontakte* **1991**, 55. (d) Hirschmann, R. *Angew. Chem., Int. Ed. Engl.* **1991**, *30*, 1278. (e) Olson, G. L.; Bolin, D. R.; Bonner, M. P.; Bös, M.; Cook, C. M.; Fry, D. C.; Graves, B. J.; Hatada, M.; Hill, D. E.; Kahn, M.; Madison, V. S.; Rusiecki, V. K.; Sarabu, R.; Sepinwall, J.; Vincent, G. P.; Voss, M. E. *J. Med. Chem.* **1993**, *36*, 3039. (f) Wiley, R. A.; Rich, D. H. *Med. Res. Rev.* **1993**, *13*, 327. (g) Chorev, M.; Goodman, M. *Acc. Chem. Res.* **1993**, *26*, 266. (h) Zuckermann, R. N. *Curr. Opin. Struct. Biol.* **1993**, *3*, 580. (i) Kahn, M. *Synlett* **1993**, 821. (j) Giannis, A.; Kolter, T. *Angew. Chem., Int. Ed. Engl.* **1993**, *32*, 1244. (k) Gante, J. *Angew. Chem., Int. Ed. Engl.* **1994**, *33*, 1699. (l) Liskamp, R. M. J. *Recl. Trav. Chim. Pays-Bas* **1994**, *113*, 1. (m) Adang, A. E. P.; Hermkens, P. H. H.; Linders, J. T. M.; Ottenheijm, H. C. J.; van Staveren, C. J. *Recl. Trav. Chim. Pays-Bas* **1994**, *113*, 63. (n) Beeley, N. *Trends Biotechnol.* **1994**, *12*, 213. (o) Schneider, J. P.; Kelly, J. W. *Chem. Rev.* **1995**, *95*, 2169. (p) Goodman, M.; Shao, H. *Pure Appl. Chem.* **1996**, *68*, 1303. (q) Nowick, J. S.; Smith, E. M.; Pairish, M. *Chem. Soc. Rev.* **1996**, *25*, 401.

(2) (a) Kemp, D. S.; Bowen, B. R. In *Tetrahedron Lett.* **1988**, *29*, 5077. (b) Kemp, D. S.; Bowen, B. R. *Tetrahedron Lett.* **1988**, *29*, 5081. (c) Kemp, D. S.; Bowen, B. R.; Muendel, C. C. *J. Org. Chem.* **1990**, *55*, 4650.

(3) (a) Kemp, D. S.; Bowen, B. R. In *Protein Folding: Deciphering the Second Half of the Genetic Code*; Gierasch, L. M., King, J., Eds.; American Association for the Advancement of Science: Washington, DC, 1990; pp 293−303. (b) Kemp, D. S.; Muendel, C. C.; Blanchard, D. E.; Bowen, B. R. In *Peptides: Chemistry, Structure and Biology: Proceedings of the Eleventh American Peptide Symposium*; Rivier, J. E., Marshall, G. R., Eds.; ESCOM: Leiden, 1990; pp 674−676. (c) Kemp, D. S.; Blanchard, D. E.; Muendel, C. C. In *Peptides: Chemistry, Structure and Biology: Proceedings of the Twelfth American Peptide Symposium*; Smith, J. A., Rivier, J. E., Eds.; ESCOM: Leiden, 1992; pp 319−322.

(4) (a) Martin, S. F.; Austin, R. E.; Oalmann, C. J. *Tetrahedron Lett.* **1990**, *31*, 4731. (b) Martin, S. F.; Austin, R. E.; Oalmann, C. J.; Baker, W. R.; Condon, S. L.; deLara, E.; Rosenberg, S. H.; Spina, K. P.; Stein, H. H.; Cohen, J.; Kleinert, H. D. *J. Med. Chem.* **1992**, *35*, 1710. (c) Baker, W. R.; Jae, H.-S.; Martin, S. F.; Condon, S. L.; Stein, H. H.; Cohen, J.; Kleinert, H. D. *Bioorg. Med. Chem. Lett.* **1992**, *2*, 1405. (d) Martin, S. F.; Oalmann, C. J.; Liras, S. *Tetrahedron* **1993**, *49*, 3521.

(5) (a) Smith, A. B., III; Keenan, T. P.; Holcomb, R. C.; Sprengeler, P. A.; Guzman, M. C.; Wood, J. L.; Carroll, P. J.; Hirschmann, R. *J. Am. Chem. Soc.* **1992**, *114*, 10672. (b) Smith, A. B., III; Holcomb, R. C.; Guzman, M. C.; Keenan, T. P.; Sprengeler, P. A.; Hirschmann, R. *Tetrahedron Lett.* **1993**, *34*, 63. (c) Smith, A. B., III; Hirschmann, R.; Pasternak, A.; Akaishi, R.; Guzman, M. C.; Jones, D. R.; Keenan, T. P.; Sprengeler, P. A.; Darke, P. L.; Emini, E. A.; Holloway, M. K.; Schleif, W. A. *J. Med. Chem.* **1994**, *37*, 215. (d) Smith, A. B., III; Guzman, M. C.; Sprengeler, P. A.; Keenan, T. P., Holcomb, R. C.; Wood, J. L.; Carroll, P. J.; Hirschmann, R. *J. Am. Chem. Soc.* **1994**, *116*, 9947. (e) Smith, A. B.; Akaishi, R.; Jones, D. R.; Keenan, T. P.; Guzman, M. C.; Holcomb, R. C.; Sprengeler, P. A.; Wood, J. L.; Hirschmann, R.; Holloway, M. K. *Biopolymers* **1995**, *37*, 29. (f) Smith, A. B.; Hirschmann, R.; Pasternak, A.; Guzman, M. C.; Yokoyama, A.; Sprengeler, P. A.; Darke, P. L.; Emini, E. A.; Schleif, W. A. *J. Am. Chem. Soc.* **1995**, *117*, 11113.

S0002-7863(96)03843-7 CCC: $14.00 

related to Kemp's 2,8-diaminoepindolidione, mimics a $\beta$-strand and induces a $\beta$-strand conformation in an adjacent peptide strand.[6] Molecules designed as peptidomimetic decoys that duplicate a portion of the intracellular adhesion molecule 1 (ICAM-1) and contain the 3-amino-4(*1H*)-quinoline template were synthesized; however, the desired biological activity was not detected. Pallai, Rebek, and co-workers described bicyclic vinylamides, which mimic aspects of the main-chain and side-chain functionality of a peptide $\beta$-strand, and used these molecules to mimic a four-residue segment of the CD4 receptor.[7] Very recently, Schrader and Kirsten reported that 3-aminopyrazole stabilizes a $\beta$-strand conformation in dipeptides by means of intermolecular hydrogen bonding.[8] Many other peptidomimetic compounds that duplicate different aspects of peptide strand structure have been developed. These include azapeptides,[9] vinylogous polypeptides,[10] azatides,[11] and various other unnatural biopolymers.[12]

Several years ago, we became interested in combining $\beta$-strand mimics, other peptidomimetic templates, and peptide strands to create compounds that mimic the structure and hydrogen-bonding patterns of $\beta$-sheets. We envision these *artificial* $\beta$-sheets as model systems in which to study $\beta$-sheet structure and stability.[1q,13] From these model studies, we hope to gain insight into protein folding, enzyme−substrate interactions, and $\beta$-amyloid deposition in Alzheimer's disease. We are also interested in developing artificial $\beta$-sheets as building blocks for molecular receptors and catalysts.

Since 1992, we have reported the development of peptidomimetic templates, which we have termed *molecular scaffolds*.[14] These templates are based upon a simple oligourea structure and resemble, in some ways, $\beta$-turns. The oligourea molecular scaffolds are designed to hold two or more peptide strands in proximity and induce the formation of hydrogen-bonded $\beta$-sheet structures. In 1995, we reported an artificial parallel $\beta$-sheet containing a diurea molecular scaffold and two attached peptide strands.[15] Early in 1996, we described artificial antiparallel $\beta$-sheet **1**, in which 5-amino-2-methoxybenzamide $\beta$-strand mimic **A** and a diurea molecular scaffold stabilize $\beta$-sheet structure in an attached peptide strand.[16]

With the goal of preparing larger artificial $\beta$-sheets, we required an extended $\beta$-strand mimic. We wanted the $\beta$-strand mimic to duplicate the hydrogen-bonding functionality of one edge of a peptide $\beta$-strand and lack hydrogen-bonding functionality along the other edge. None of the $\beta$-strand mimics

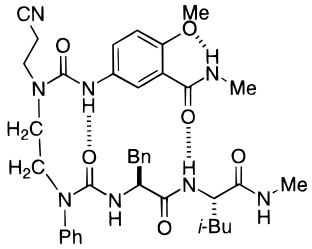

artificial β-sheet **1**

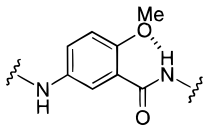

β-strand mimic **A**

developed by other researchers meets these requirements. $\beta$-Strand mimic **A** provides the right pattern of hydrogen-bonding groups along one edge and is blocked along the other edge, but it is too short. We reasoned that it might be possible to extend the 5-amino-2-methoxybenzamide $\beta$-strand mimic by linking two or more of these units end-to-end, by the nitrogen atoms, to generate 5-hydrazino-2-methoxybenzoic acid $\beta$-strand mimic **B**. This paper reports the development of this extended $\beta$-strand mimic and its successful application to the creation of artificial $\beta$-sheet **2**.

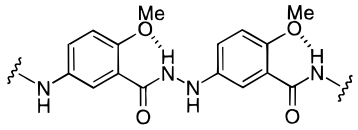

β-strand mimic **B**

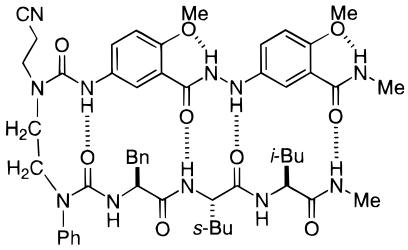

artificial β-sheet **2**

## Results and Discussion

The first half of this section describes synthetic and structural studies of methoxy-substituted derivatives of hydrazinobenzoic acid. These studies establish that hydrazide derivatives of 5-hydrazino-2-methoxybenzoic acid adopt a conformation similar to that of a peptide $\beta$-strand and are suitable for use as $\beta$-strand mimics. The second half describes the coupling of 5-hydrazino-2-methoxybenzoic acid $\beta$-strand mimic **B** to a tripeptide strand by means of an ethylenediamine diurea molecular scaffold to form artificial $\beta$-sheet **2**. Structural studies indicate that **2** adopts a hydrogen-bonded conformation similar to that of an antiparallel $\beta$-sheet and establish that $\beta$-strand mimic **B** can induce $\beta$-sheet formation in an attached peptide strand.

**Design of the $\beta$-Strand Mimic.** We envisioned *m*-hydrazinobenzoic acid as a building block for extended $\beta$-strand mimics. If the hydrazinobenzoic acid units are coupled by means of hydrazide linkages, an oligomeric $\beta$-strand mimic is formed. In this oligomer, each hydrazinobenzoic acid unit is equivalent in length to the main-chain of a dipeptide (six atoms), and the C═O and NH groups are in the same positions as the C═O and NH groups of one edge of a peptide $\beta$-strand. Chart 1 shows the relationship between this oligomer and a peptide strand; key hydrogen-bonding groups are highlighted in boldface.

(6) Michne, W. F.; Schroeder, J. D. *Int. J. Peptide Protein Res.* **1996**, *47*, 2.
(7) Boumendjel, A.; Roberts, J. C.; Hu, E.; Pallai, P. V.; Rebek, J., Jr. *J. Org. Chem.* **1996**, *61*, 4434.
(8) Schrader, T.; Kirsten, C. *Chem. Commun.* **1996**, 2089.
(9) Gante, J. *Synthesis* **1989**, 405.
(10) Hagihara, M.; Anthony, N. J.; Stout, T. J.; Clardy, J.; Schreiber, S. L. *J. Am. Chem. Soc.* **1992**, *114*, 6568.
(11) Han, H.; Janda, K. D. *J. Am. Chem. Soc.* **1996**, *118*, 2539.
(12) (a) Liskamp, R. M. J. *Angew. Chem., Int. Ed. Engl.* **1994**, *33*, 633. (b) Moran, E. J.; Wilson, T. E.; Cho, C. Y.; Cherry, S. R.; Schultz, P. G. *Biopolymers* **1995**, *37*, 213.
(13) (a) Nowick, J. S.; Lee, I. Q.; Mackin, G.; Pairish, M.; Shaka, A. J.; Smith, E. M.; Ziller, J. W. In *Molecular Design and Bioorganic Catalysis*; Wilcox, C. S., Hamilton, A. D., Eds.; Kluwer Academic: Dordrecht, Netherlands, 1996; pp 111−136. (b) Smith, E. M.; Pairish, M.; Nowick, J. S. In *Self-Assembly in Synthetic Chemistry*; Wuest, J. D., Ed.; Kluwer Academic: Dordrecht, Netherlands, in press.
(14) (a) Nowick, J. S.; Powell, N. A.; Martinez, E. J.; Smith, E. M.; Noronha, G. *J. Org. Chem.* **1992**, *57*, 3763. (b) Nowick, J. S.; Abdi, M.; Bellamo, K. A.; Love, J. A.; Martinez, E. J.; Noronha, G.; Smith, E. M.; Ziller, J. W. *J. Am. Chem. Soc.* **1995**, *117*, 89. (c) Nowick, J. S.; Mahrus, S.; Smith, E. M.; Ziller, J. W. *J. Am. Chem. Soc.* **1996**, *118*, 1066.
(15) Nowick, J. S.; Smith, E. M.; Noronha, G. *J. Org. Chem.* **1995**, *60*, 7386.
(16) Nowick, J. S.; Holmes, D. L.; Mackin, G.; Noronha, G.; Shaka, A. J.; Smith, E. M. *J. Am. Chem. Soc.* **1996**, *118*, 2764.

**Chart 1**

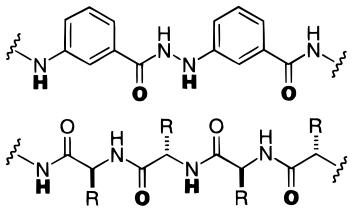

**Chart 2**

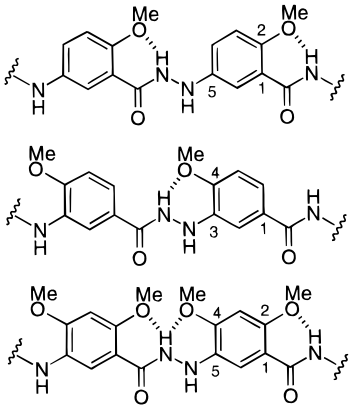

**Scheme 1**

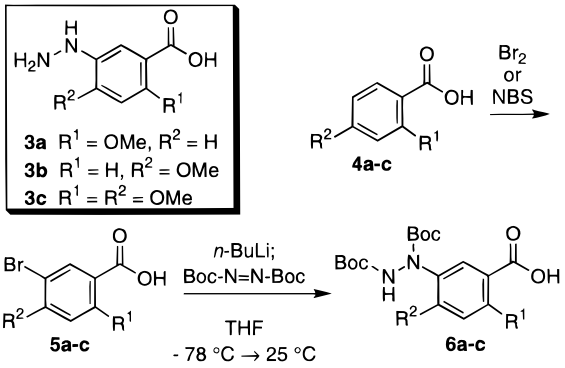


We hypothesized that methoxy substitutuents ortho to either the carboxyl group, the hydrazino group, or both might enforce an extended conformation by means of intramolecular hydrogen bonding. Thus, we considered oligomers of 5-hydrazino-2-methoxybenzoic acid, 3-hydrazino-4-methoxybenzoic acid, and 5-hydrazino-2,4-dimethoxybenzoic acid for further study. Chart 2 illustrates these structures and the hypothesized patterns of hydrogen bonding.

The Cambridge Structural Database provided us with insight into some of the features of these structures. 2-Methoxybenzamides adopt intramolecularly hydrogen bonded conformations. Various hydrazides in the database adopt either a linear or a twisted geometry about the N−N bond. No data on the effect of *o*-methoxy substituents upon the conformation of aromatic hydrazides is available. To gain further insight into the structures of methoxy-substituted *m*-hydrazinobenzoic acid derivatives, we turned to synthetic and structural studies.

**Synthesis of Hydrazinobenzoic Acid Derivatives.** Derivatives of 5-hydrazino-2-methoxybenzoic acid (**3a**), 3-hydrazino-4-methoxybenzoic acid (**3b**), and 5-hydrazino-2,4-dimethoxybenzoic acid (**3c**) were prepared for further study. These compounds were synthesized from commercially available 2-methoxy-, 4-methoxy-, and 2,4-dimethoxybenzoic acids **4a**−**c** as shown in Scheme 1. The 2- and 4-methoxybenzoic acids were brominated using bromine; the 2,4-dimethoxy compound was brominated using *N*-bromosuccinimide (NBS).[17] Halogen−metal exchange using 2−3 equiv of *n*-butyllithium, followed by reaction of the resulting organolithium compounds with di-*tert*-butylazodicarboxylate, gave di-*tert*-butyloxycarbonyl (Boc) protected hydrazinobenzoic acids **6a**−**c**.[18] Although the conversions proceed in modest yields (typically 30−50%), the 5-hydrazino-2-methoxybenzoic acid derivative (**6a**) is readily purified to analytical purity by precipitation and washing, making its preparation especially convenient. $^1$H NMR analysis of **6a**−**c** is complicated by the presence of multiple conformers that interconvert slowly on the NMR time scale. The Boc-protected derivatives **6a**−**c** can be converted to hydrazinobenzoic acids **3a**−**c** (as the mono- or dihydrochloride salts) by treatment with a mixture of concentrated aqueous HCl and isopropyl alcohol. The $^1$H NMR spectra of these salts show single conformers, simplifying their spectroscopic analysis.

**Table 1.** Spectroscopic Properties of NH Groups of Hydrazides **7** and **8** (22 °C, 10 mM in $CHCl_3$ or $CDCl_3$)

| | IR ($cm^{-1}$) | | $^1$H NMR (ppm) | |
|---|---|---|---|---|
| compd | $NH_a$ | $NH_b$ | $H_a$ | $H_b$ |
| **7a** | 3436 | 3329 | 7.94 | 6.30 |
| **7b** | 3437 | 3344 | 7.95 | 6.79 |
| **7c** | 3437 | 3338 | 7.89 | 6.62 |
| **8a** | 3402 | 3336 | 9.45 | 6.40 |
| **8b** | 3402 | 3352 | 9.43 | 6.85 |
| **8c** | 3404 | 3342 | 9.43 | 6.71 |

**IR and $^1$H NMR Spectroscopic Studies of Hydrazinobenzoic Acid Derivatives.** Hydrazides **7a**−**c** and **8a**−**c** were synthesized and studied spectroscopically, to determine the effects of methoxy substituents on the conformations of *m*-hydrazinobenzoic acid derivatives. *tert*-Butyloxycarbonyl compounds **6a**−**c** were converted to hydrazides **7a**−**c** and **8a**−**c** by successive methyl esterification with diazomethane, removal of the *tert*-butyloxycarbonyl groups with HCl, and acylation with either benzoyl chloride or *o*-anisoyl chloride.

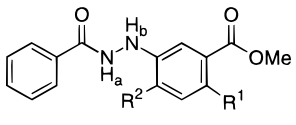

**7a** $R^1$ = OMe, $R^2$ = H
**7b** $R^1$ = H, $R^2$ = OMe
**7c** $R^1$ = $R^2$ = OMe

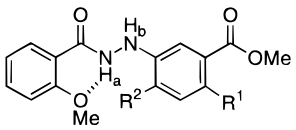

**8a** $R^1$ = OMe, $R^2$ = H
**8b** $R^1$ = H, $R^2$ = OMe
**8c** $R^1$ = $R^2$ = OMe

Compounds **7** and **8** exhibit significant differences in their infrared and $^1$H NMR spectra in $CHCl_3$ or $CDCl_3$ solution (Table 1). These studies were performed at 10 mM, a concentration at which little or no self-association occurs. In the infrared spectrum, the amidic $NH_a$ stretch appears as a band centered at ca. 3437 $cm^{-1}$ in benzoyl derivatives **7a**−**c**, and at ca. 3403 $cm^{-1}$ in *o*-anisoyl derivatives **8a**−**c**. The weakened NH stretch in *o*-anisoyl derivatives **8** provides evidence that the *o*-methoxy group of the anisoyl fragment is hydrogen bonded to the amide NH group. In the $^1$H NMR spectrum, the amidic $NH_a$ group appears at 7.89−7.95 ppm in **7a**−**c** and at 9.43−9.45 ppm in **8a**−**c**. The substantial downfield shift of this resonance in **8a**−**c** provides further evidence for hydrogen bonding of the *o*-methoxy group.

The IR stretching frequencies of the $NH_a$ groups of compounds **7a**−**c** differ little, as do the $^1$H NMR chemical shifts of $H_a$ in these molecules. The IR and $^1$H NMR properties of $H_a$

(17) Auerbach, J.; Weissman, S. A.; Blacklock, T. J.; Angeles, M. R.; Hoogsteen, K. *Tetrahedron Lett.* **1993**, *34*, 931.
(18) Demers, J. P.; Klaubert, D. H. *Tetrahedron Lett.* **1987**, *28*, 4933.

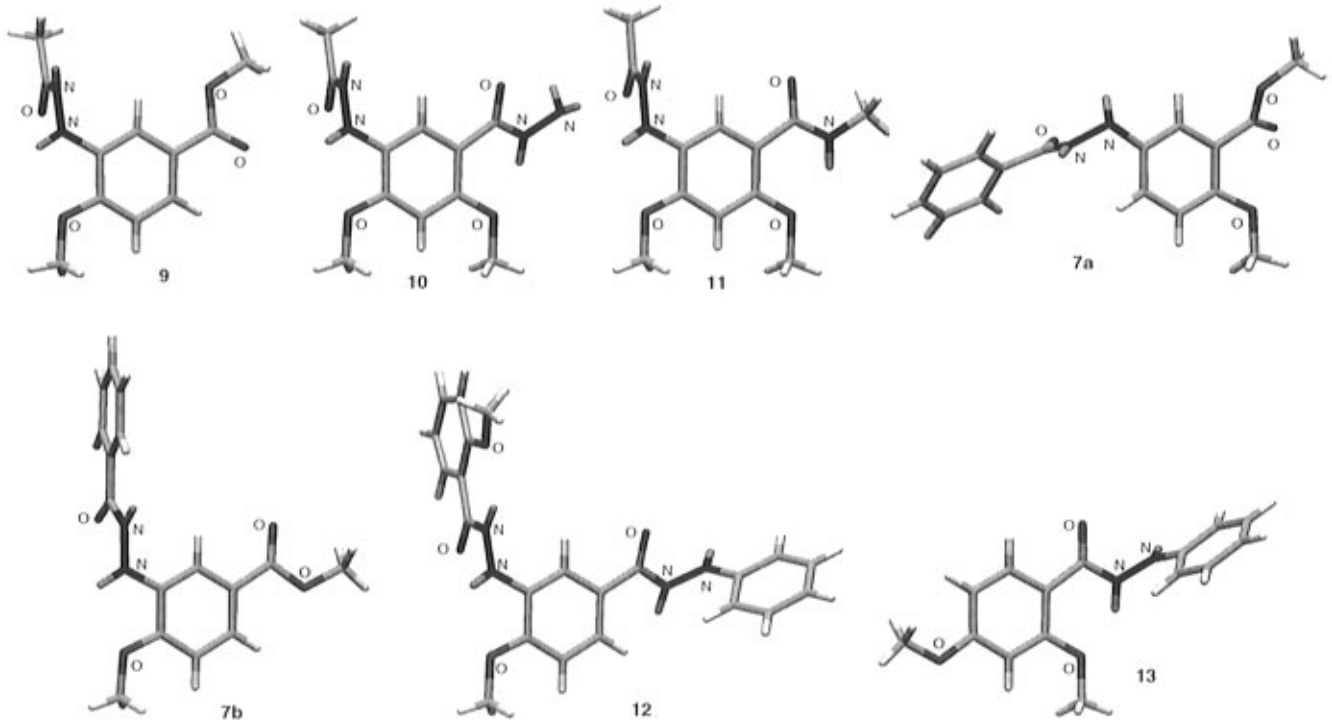


**Figure 1.** X-ray crystallographic structures of hydrazides **7a,b** and **9**−**13**. Hydrazide **7b** has three crystallographically-independent molecules per asymmetric unit. The molecules differ little in geometry, and only one is shown above. Hydrazide **11** has two crystallographically-independent molecules per asymmetric unit. The molecules differ little in geometry, and only one is shown above.

in compounds **8a**−**c** are also similar to each other. These data indicate that methoxy groups at the 4-positions ($R^2$) of these molecules do not hydrogen bond to the amidic hydrogens ($H_a$). Collectively, these IR and $^1$H NMR studies indicate that 2-methoxy groups help enforce the desired extended conformation in chloroform solution, while 4-methoxy groups do not.

**X-ray Crystallographic Studies of Hydrazinobenzoic Acid Derivatives.** X-ray crystallography provides insight into the conformations of the methoxy-substituted hydrazinobenzoic acid derivatives in the solid state. We prepared and attempted to crystallize a variety of methoxy-substituted *m*-hydrazinobenzoic acid derivatives. Of these derivatives, compounds **7a**, **7b**, and **9**−**13** afforded crystals suitable for X-ray crystallography. The X-ray crystallograpic structures of these compounds are shown in Figure 1.

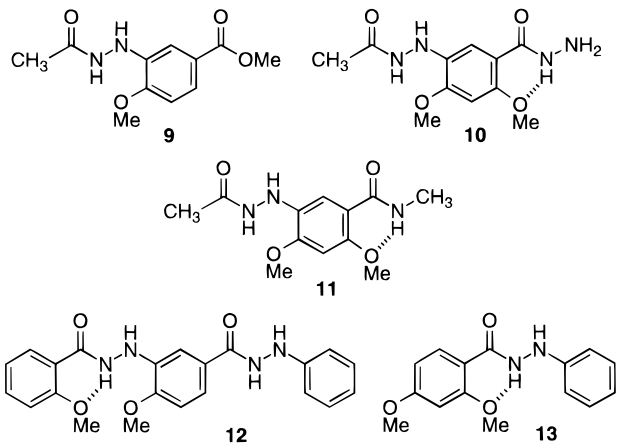


Three trends are evident from these structures. The hydrazide groups are twisted, with C−N−N−C torsion angles ranging from 70° to 97°. Structure **a** in Chart 3 summarizes this finding pictorially. When a methoxy group is at the 2-position of an aromatic ring, an amide group at the 1-position is hydrogen bonded to this group (Chart 3, structure **b**). When a methoxy group is at the 4-position of an aromatic ring, a hydrazide group at the 3- or 5-position is rotated so that the amine NH group is directed toward the methoxy group (Chart 3, structure **c**). These observations are consistent with the solution-phase studies described above and indicate that methoxy substitution at the 2-position of the hydrazinobenzoic acids stabilizes a desired conformation, while methoxy substitution at the 4-position stabilizes an undesired conformation.

**Chart 3**

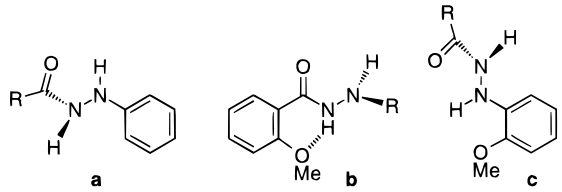


X-ray crystallography provides insight into the hydrogen-bonding properties of the hydrazinobenzoic acid derivatives as well as their conformations. Thus, hydrazide derivatives **7a**, **12**, and **13** form hydrogen-bonded dimers in which two molecules are antiparallel to each other, and the carbonyl oxygen atoms and the amine NH groups participate in hydrogen-bonded ten-membered rings (Figure 2). Because of the antiparallel orientations of the molecules and the geometry of the hydrogen-bonded rings, these dimers resemble antiparallel $\beta$-sheets. In each of these dimers, the amine groups lack ortho methoxy substitution. In contrast, hydrazides **7b**, **9**, **10**, and **11** do not form hydrogen-bonded dimers of this sort and have methoxy substituents ortho to the amine NH of the hydrazide group. These observations indicate that methoxy-substituted *m*-hydrazinobenzoic acid derivatives form $\beta$-sheetlike hydrogen-bonded dimers if there is a methoxy substituent at the 2-position, but not if there is a methoxy substituent at the 4-position. The X-ray studies as well as the IR and $^1$H NMR studies indicate that the 5-hydrazino-2-methoxybenzoic acid building block may

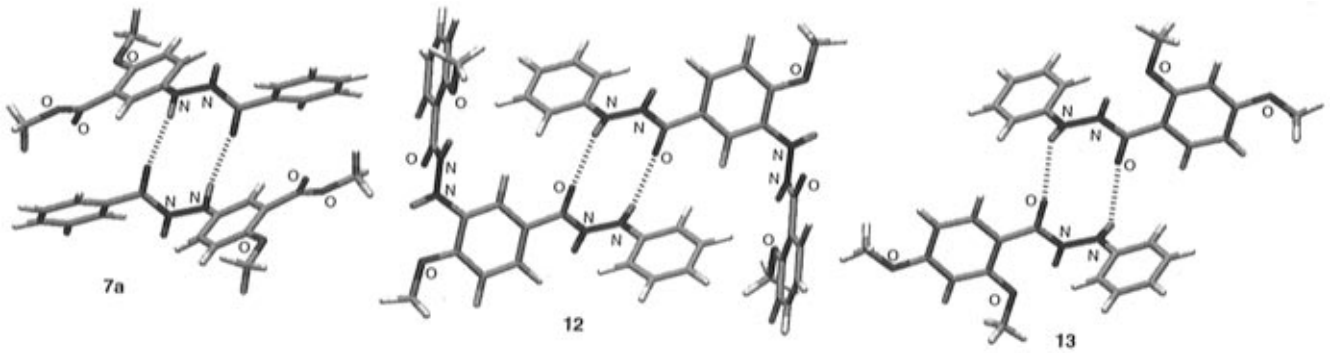


**Figure 2.** Hydrogen-bonded dimers in the X-ray crystallographic structures of hydrazides **7a**, **12**, and **13**.

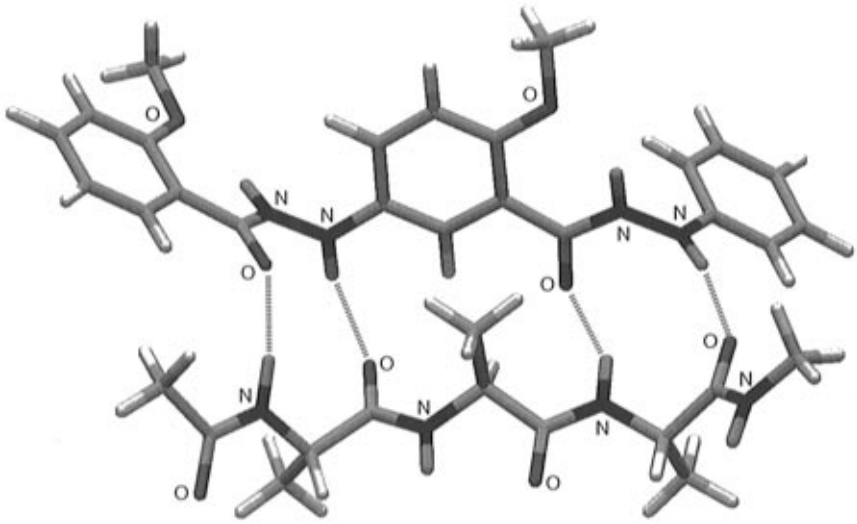

**Figure 3.** Model of a peptide strand docked to hydrazide **14**. The model for hydrazide **14** was generated from the crystallographic coordinates of **7a** with C−N−N−C torsion angles of −82° and 82°, respectively. The geometry of **14** was held fixed, while Ac-Ala-Ala-Ala-NHMe was docked to it and energy minimized using MacroModel V5.0 with the AMBER* force field.

be suitable for use as a β-strand mimic, while the 3-hydrazino-4-methoxybenzoic acid and 5-hydrazino-2,4-dimethoxybenzoic acid building blocks are not.

**Molecular Modeling Studies.** Many other hydrazides that were prepared did not yield crystals suitable for X-ray crystallography. Of these, we were particularly interested in hydrazide **14**, because the IR, $^1$H NMR, and X-ray crystallographic studies

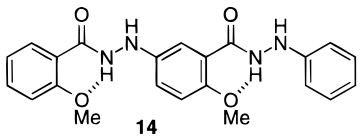

**14**

of hydrazides **7**−**13** suggested that it should adopt a β-strand conformation and be complementary to a tripeptide in length and hydrogen-bonding functionality. In the absence of a crystallographic structure of this compound, we turned to molecular modeling to predict its structure and examine its complementarity to peptides.

Molecular mechanics calculations using MacroModel V5.0 and the AMBER* force field predict the hydrazide groups of **14** to have 180° C−N−N−C dihedral angles. Adequate parameters for this group are lacking, however, and this value is unreliable in light of the overwhelming body of crystallographic evidence that a geometry of ca. 80° or 90° is preferred. Ab initio calculations on *N*′-phenylformohydrazide (PhNHNHCHO) at the 6-31G* level using Spartan corroborate the crystallographic studies and indicate that a 90° C−N−N−C dihedral angle is preferred.

Using the crystallographic coordinates of **13**, we created a model for **14** with C−N−N−C torsion angles of −82° and 82°, respectively. In this model, the distance between the carbonyl groups is 7 Å, which is comparable to that of a peptide in a β-strand conformation. Docking a peptide strand (Ac-Ala-Ala-Ala-NHMe) to this model reveals excellent complementarity between the peptidomimetic template and the peptide strand; after energy minimization, the peptide strand adopts a β-strand conformation and hydrogen bonds to the template (Figure 3). These modeling studies suggest that hydrazide derivatives of 5-hydrazino-2-methoxybenzoic acid are suitable templates for inducing a β-strand conformation in peptides.

**Synthesis of Artificial β-Sheet 2.** To further evaluate the 5-hydrazino-2-methoxybenzoic acid template, we combined this unit with a 1,2-diaminoethane diurea molecular scaffold and a tripeptide strand to form artificial β-sheet **2**. Artificial β-sheet **2** was synthesized as shown in Scheme 2. Amine **15** was converted to urea **16** by reaction with phenylalanylisoleucylleucine methyl ester isocyanate[19] and subsequent aminolysis of the peptide methyl ester group by treatment with methylamine in methanol. The Boc protective group was removed by treatment with HCl in methanol, and the free amine was formed upon treatment of the resulting amine hydrochloride salt with aqueous base. Reaction with isocyanate **17** then afforded urea **18**. Hydrogenolysis of the benzyl ester protective group, followed by coupling of the resulting carboxylic acid with *N*-methyl-5-hydrazino-2-methoxybenzamide hydrochloride (**19**) using 1-ethyl-

(19) Nowick, J. S.; Holmes, D. L.; Noronha, G.; Smith, E. M.; Nguyen, T. M.; Huang, S.-L. *J. Org. Chem.* **1996**, *61*, 3929.

**Scheme 2**

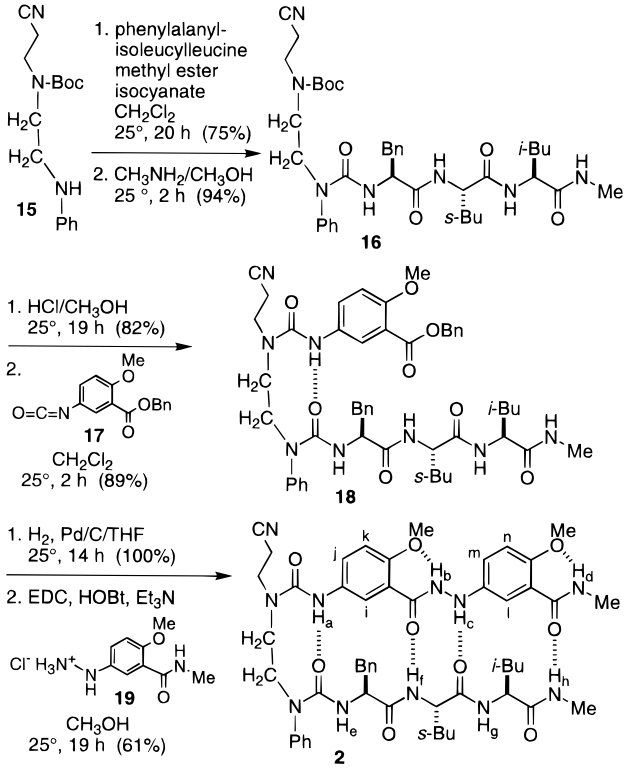


3-(3′-dimethylaminopropyl)carbodiimide hydrochloride (EDC), generated the artificial $\beta$-sheet. Artificial $\beta$-sheet **2** was subsequently prepared by solid-phase synthesis on Merrifield resin using a slightly modified version of the route shown in Scheme 2. This procedure will be described in a forthcoming paper on the solid-phase synthesis of artificial $\beta$-sheets.[20]

**$^1$H NMR Chemical Shift Studies of Artificial $\beta$-Sheet 2.** $^1$H NMR chemical shift studies indicate that **2** forms a hydrogen-bonded antiparallel $\beta$-sheet structure in $CDCl_3$ solution. In these studies, the chemical shifts of the NH groups of artificial $\beta$-sheet **2** were compared to those of analogous protons in compounds **20** and **21**. These two compounds serve as controls, resembling respectively the upper (peptidomimetic) and lower (peptide) halves of artificial $\beta$-sheet **2**.

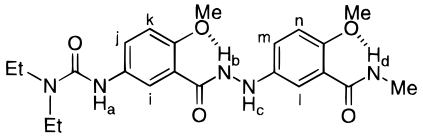


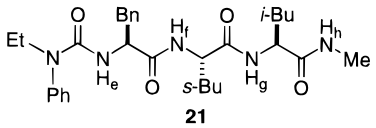


In 1 mM $CDCl_3$ solution, protons $H_a$, $H_c$, $H_f$, and $H_h$ appear 1.15−3.68 ppm downfield of the analogous protons of controls **20** and **21** (Table 2).[21] In this solvent, hydrogen-bonded NH protons generally appear about 2−3 ppm downfield of NH protons that are not hydrogen bonded. Thus, non-hydrogen-bonded aliphatic amide protons generally appear at about 6 ppm, while hydrogen-bonded aliphatic amide protons generally appear at about 8 ppm.[15,16] The chemical shifts of $H_f$ and $H_h$ of artificial $\beta$-sheet **2** (8.14 and 8.02 ppm) suggest that these protons are fully hydrogen bonded and that **2** predominantly adopts a hydrogen-bonded $\beta$-sheet conformation. Amide proton $H_g$ appears at 6.07 ppm in **2**, indicating that it is not hydrogen bonded. In control **21**, however, $H_g$ appears downfield at 7.52 ppm. We interpret the shift of $H_g$ in **21** to mean that it forms a hydrogen-bonded $\beta$-turn with the carbonyl of the urea group (vide infra), a phenomenon which we have observed in other peptide ureas.[15,16] In summary, these shift data suggest that in **2** the $\beta$-strand mimic hydrogen bonds to the peptide strand, forcing it to adopt an extended conformation and preventing it from adopting a hydrogen-bonded $\beta$-turn conformation.

**Table 2.** $^1$H NMR Chemical Shifts of the NH Protons of **2**, **20**, and **21** (30 °C, 1 mM in $CDCl_3$)

| | $H_a$ | $H_b$ | $H_c$ | $H_d$ | $H_e$ | $H_f$ | $H_g$ | $H_h$ |
|---|---|---|---|---|---|---|---|---|
| **2** | 9.95 | 9.55 | 8.45 | 8.10 | 4.80 | 8.14 | 6.07 | 8.02 |
| **20** | 6.27 | 9.54 | 6.41 | 7.87 | | | | |
| **21** | | | | | 4.50 | 6.48 | 7.52 | 6.87 |

**Table 3.** $^1$H NMR Chemical Shifts of the Aromatic Protons of **2** and **20** (30 °C, 1 mM in $CDCl_3$)

| | $H_i$ | $H_j$ | $H_k$ | $H_l$ | $H_m$ | $H_n$ |
|---|---|---|---|---|---|---|
| **2** | 8.66 | 8.40 | 6.98 | 8.16 | 7.07 | 6.90 |
| **20** | 7.66 | 8.08 | 6.99 | 7.84 | 7.02 | 6.88 |

The aromatic ring protons of artificial $\beta$-sheet **2** also differ in chemical shift from those of control **20**. $\beta$-Strand mimic proton $H_i$ of artificial $\beta$-sheet **2** is shifted 1.00 ppm downfield of the corresponding proton in control **20** (Table 3). The downfield shifting of both this proton and $H_a$ apparently results from proximity to the carbonyl group of the urea on the bottom half of **2**; that the shifts are exceptionally large suggests that the carbonyl group is exceptionally close to both protons.[22] $\beta$-Strand mimic protons $H_j$ and $H_l$ are each shifted downfield by 0.32 ppm in **2**. These shifts may reflect enforced proximity to the carbonyl groups of the upper urea and the isoleucine. Similar downfield shifting has been observed in other peptidomimetic $\beta$-sheets,[1a,3] and in protein $\beta$-sheets,[23] and may also reflect proximity of carbonyl groups in these compounds.

**$^1$H NMR NOE Studies of Artificial $\beta$-Sheet 2.** $^1$H NMR nuclear Overhauser effect (NOE) studies indicate that the peptidomimetic and peptide strands of **2** are near each other and provide strong evidence that **2** adopts an antiparallel $\beta$-sheet conformation in $CDCl_3$ solution.[24] At 500 MHz and 21 °C, **2** exhibits very small NOEs, presumably as a result of its high molecular weight (989). At 30 °C, the NOEs are larger, however, allowing us to perform a series of 1-D NOE studies, in which 22 of the molecule's 39 distinct resonances were irradiated, and 83 NOEs were observed and quantified. In these experiments, most of the NOEs detected were between 1 and 4%, and it was possible to be confident that NOEs of 0.4% or greater were real rather than artifacts. These studies are discussed below and are described in detail in the Experimental

(20) Holmes, D. L.; Smith, E. M.; Nowick, J. S. Submitted to *J. Am. Chem. Soc.*

(21) Under the conditions of these studies, compounds **2**, **20**, and **21** do not self-associate to any appreciable extent. Dilution titration studies indicate that these compounds self-associate with dimerization constants of ca. 1 $M^{-1}$ at ambient temperature in $CDCl_3$ solution. In artificial $\beta$-sheet **2**, protons $H_g$ and $H_e$ exhibit the largest concentration-dependent changes in chemical shift. This observation suggests that these protons are most available for intermolecular hydrogen bonding and is consistent with the pattern of intramolecular hydrogen bonding seen in this compound. In controls **20** and **21**, protons $H_a$, $H_c$, $H_f$, and $H_h$ exhibit the largest concentration-dependent changes in chemical shift.

(22) Wagner, G.; Pardi, A.; Wüthrich, K. *J. Am. Chem. Soc.* **1983**, *105*, 5948.

(23) (a) Wishart, D. A.; Sykes, B. D.; Richards, F. M. *J. Mol. Biol.* **1991**, *222*, 311. (b) Wishart, D. A.; Sykes, B. D.; Richards, F. M. *Biochemistry* **1992**, *31*, 1647, and references contained therein.

(24) Wüthrich, K. *NMR of Proteins and Nucleic Acids*; Wiley: New York, 1986; pp 124−129.

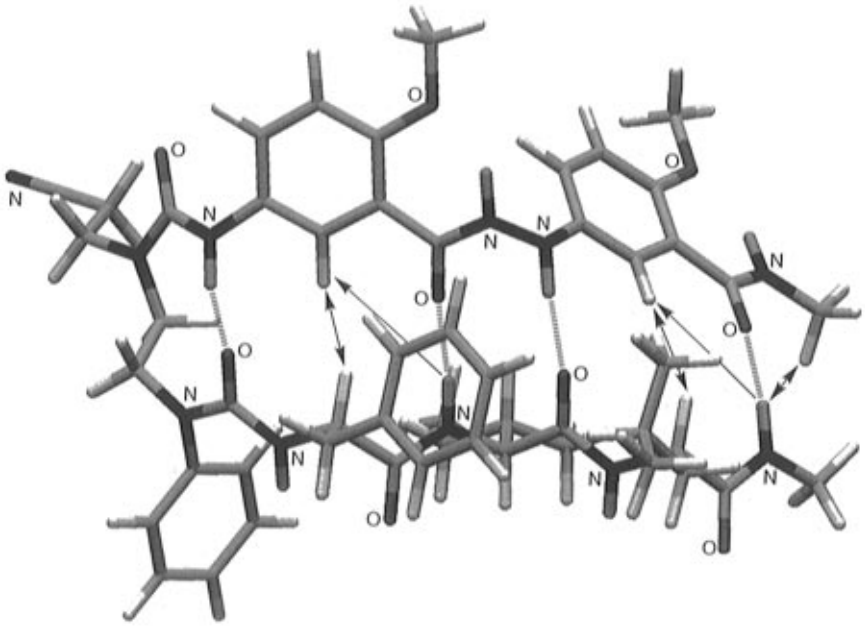

**Figure 4.** Model of artificial β-sheet **2** illustrating long-range NOEs. The model was generated using MacroModel V5.0 with the AMBER* force field. The starting geometry (before minimization) was chosen to reflect the preferred (anti) conformation of the 1,2-diaminoethane diurea backbone.[14b,c] The starting conformations of the amino acid side chains were chosen to reflect measured coupling constants and NOEs when possible but are largely arbitrary. Adequate parameters for the C−N−N−C torsion angle of the hydrazide group were not available, and this torsion was constrained to the crystallographically observed value of 80° during minimization. Only small differences in the hydrogen-bonded β-sheet structure occur if the C-N-N-C torsion angle is varied; in other modeling studies the angle was constrained to −80° or unconstrained (180°) with little effect upon the β-sheet structure. Mirror-image diastereomeric geometry of the N−C−C−N diurea backbone and different starting conformations of the amino acid side chains were also employed, with little effect on the β-sheet structure.

**Chart 4**

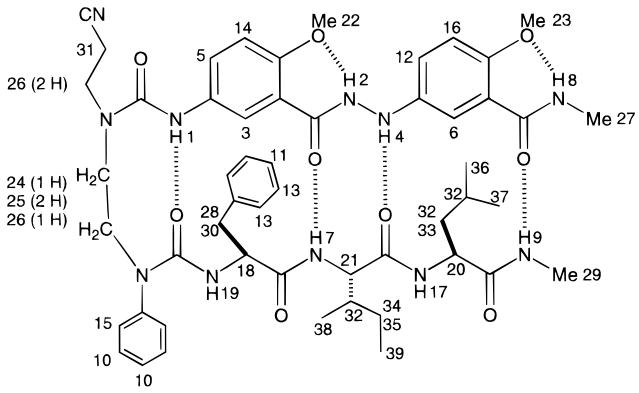

Section. Chart 4 will aid in this discussion, illustrating the 39 resonances that were observed (numbered in order of decreasing chemical shift) and showing their assignments to the various protons of **2**. These assignments were determined by means of COSY and NOE studies.

Long-range NOEs between the peptide and peptidomimetic strands of **2** provide compelling evidence for a β-sheet structure. Strong NOEs were observed between β-strand mimic proton 3 and the Phe α proton (18) and between β-strand mimic proton 6 and the Leu α proton (20). An NOE from the Ile NH (7) to β-strand mimic proton 3 and an NOE from the lower methylamide NH (9) to β-strand mimic proton 6 were also observed. In addition, there were NOEs between the lower methylamide NH (9) and the upper methylamide methyl group (27). Figure 4 provides a three-dimensional representation illustrating these NOEs. These long-range NOE data are characteristic of an antiparallel β-sheet structure and show that the peptide and peptidomimetic strands of **2** are aligned.[24]

Short-range NOEs within the peptide strand provide further evidence for β-sheet structure. Strong NOEs were observed between the Ile NH (7) and Phe α (18) protons, the Leu NH (17) and Ile α (21) protons, and the lower methylamide NH (9) and Leu α (20) protons. These interresidue NOEs are stronger than the intraresidue NOEs between the NH and α protons of these residues. Strong NOEs between the α-proton of one residue and the NH group of the next residue are characteristic of the β-strand conformation.[24] NOEs between the NH groups of the peptide strand (19, 7, 17, and 9) were not detected. The absence of these NOEs provides additional support for an extended (β-strand) conformation, in which these groups are far apart.

Short-range NOEs within the β-strand mimic indicate that this unit also adopts an extended conformation and further support the model shown in Figure 4. Thus, urea proton 1 exhibits a much stronger NOE to β-strand mimic proton 3 than to β-strand mimic proton 5; hydrazide proton 4 exhibits a stronger NOE to β-strand mimic proton 6 than to β-strand mimic proton 12; and hydrazide proton 2 exhibits a much stronger NOE to β-strand mimic proton 12 than to β-strand mimic proton 6.

A number of NOEs are not wholly consistent with the model shown in Figure 4. Urea proton 1 exhibits strong NOEs to all four protons of the 1,2-diaminoethane backbone ($NCH_2CH_2N$, 24-26). Molecular modeling indicates that the urea proton cannot be close to all four backbone protons at the same time. Instead, the backbone adopts two mirror-image diastereomeric anti conformations, each of which places two of 1,2-diaminoethane protons next to the urea NH group.[14b,c] The amino acid side-chains are also conformationally mobile. Leucine methyl group 36 exhibits small NOEs to both the phenylalanine phenyl group and to the upper methylamide methyl (27), although molecular modeling indicates that methyl 36 cannot be close to both groups at one time. The $^3J_{\alpha\beta}$ coupling constants of the Phe and Leu groups are 7−9 Hz, supporting the analysis that these sidechains have little conformational preference. These studies show that parts of artificial β-sheet **2** are conformation-

**Table 4.** Temperature Dependence of the $^1$H NMR Chemical Shifts (ppb/K) of the NH Protons of **2**, **20**, and **21** (1 mM in $CDCl_3$)[a]

| | $H_a$ | $H_b$ | $H_c$ | $H_d$ | $H_e$ | $H_f$ | $H_g$ | $H_h$ |
|---|---|---|---|---|---|---|---|---|
| **2** | −1.5 | −2.2 | −3.3 | −3.1 | −0.5 | −2.1 | −2.7[b] | −8.5 |
| **20** | −1.6 | −3.1 | −0.3 | −3.5 | | | | |
| **21** | | | | | −0.6 | −0.8[b] | −6.8 | −4.2 |

[a] Spectra recorded at 10 °C intervals from −30 °C to 30 °C. [b] Temperature-dependence of these NH shift data exhibited poor linear correlation.

ally mobile and that no single structure (e.g., Figure 4) can provide a complete picture of this molecule.

**Variable-Temperature $^1$H NMR Studies of Artificial *β*-Sheet 2.** The temperature dependence of the $^1$H NMR chemical shifts of amide NH protons reflects their state of hydrogen bonding. In $CDCl_3$, peptide amide protons that are either *not hydrogen bonded* or *locked in a hydrogen-bonded conformation* exhibit small temperature dependencies in chemical shifts, while protons that participate in an equilibrium between a hydrogen-bonded state and a non-hydrogen-bonded state exhibit large temperature dependencies in their chemical shifts.[25,26] Temperature dependencies are typically −2 or −3 ppb/K in the former case and −4 to −8 ppb/K in the latter.

In artificial *β*-sheet **2**, all protons exhibit small temperature dependencies of chemical shifts, with the exception of methylamide proton $H_h$ (Table 4). These observations are consistent with a model in which artificial *β*-sheet **2** adopts a hydrogen-bonded *β*-sheet conformation, but where the hydrogen bond to the leucine methylamide NH proton "frays" upon warming. We hesitate to place too much emphasis on the interpretation of these data: much of what is known about temperature dependence of NH shifts has been established for peptide amide NH groups, but **2** contains not only peptide amide NH groups but also urea, amine, and aromatic amide NH groups.

In controls **20** and **21**, NH groups $H_a$−$H_f$ exhibit small temperature dependencies. In contrast, the leucine NH ($H_g$) exhibits a large temperature dependence, and the leucine methylamide proton ($H_h$) exhibits a moderate temperature dependence. These temperature dependencies suggest that $H_g$ and $H_h$ of control **21** equilibrate between hydrogen-bonded and non-hydrogen-bonded states. The large temperature dependence of $H_g$ provides further support that it forms a hydrogen-bonded *β*-turn with the carbonyl of the urea group (vide supra).

**$^1$H NMR Coupling Constant Studies of Artificial *β*-Sheet 2.** The $^3J_{HN\alpha}$ coupling constants reflect the dihedral angle about the $C_\alpha$−NH bond of the amino acids, which in turn reflects the conformation of the amino acids in peptides and proteins. Coupling constants greater than 7 Hz are generally considered to be consistent with *β*-sheet structure, while coupling constants of less than 6 Hz are consistent with α-helical structure.[27,28]

Consistent with *β*-sheet structure, the $^3J_{HN\alpha}$ coupling constants of the Phe, Ile, and Leu of artificial *β*-sheet **2** are 7−9 Hz (Table 5, $H_e$, $H_f$, and $H_g$). These values should not be regarded as proof of *β*-sheet structure, however, since peptides lacking well-defined structures (e.g., control **21**) typically exhibit $^3J_{HN\alpha}$ coupling constants of 7−8 Hz. The coupling constants of hydrazide protons $H_b$ and $H_c$ are small (4−5 Hz) in both **2** and **21**. If the dependence of coupling constants upon dihedral angle for hydrazides is similar to that of peptides, this value may reflect that the hydrazide group is twisted, rather than linear. This geometry would be reasonably consistent with that which is observed crystallographically for hydrazides **7a**,**b** and **9**−**13**.

**Table 5.** $^1$H NMR Coupling Constants (Hz) of the NH Protons of **2**, **20**, and **21** (30 °C, 1 mM in $CDCl_3$)

| | $H_b$ | $H_c$ | $H_e$ | $H_f$ | $H_g$ |
|---|---|---|---|---|---|
| **2** | 4.0 | 4[a] | 8.5 | 9.1 | 7.2 |
| **20** | 5.1 | 5.2 | | | |
| **21** | | | *b* | 6.5 | 8.1 |

[a] Value is approximate, because peak appears as a broad doublet. [b] Value could not be determined due to overlap with phenylalanine α proton.

## Conclusions and Outlook

These studies establish that *β*-strand mimic **B** duplicates the hydrogen-bonding functionality of one edge of a peptide strand in a *β*-strand conformation and can template *β*-sheet formation in an attached peptide strand. 5-Hydrazino-2-methoxybenzoic acid *β*-strand mimic **B** provides an array of four hydrogen-bond donor and acceptor groups along its hydrogen-bonding edge. It is twice as long as 5-amino-2-methoxybenzoic acid *β*-strand mimic **A**, which has two hydrogen-bond donor and acceptor groups. It is also longer than Kemp's epindolidione *β*-strand mimic, which has three hydrogen-bond donor and acceptor groups. Because the N-to-C directionality of *β*-strand mimic **B** is opposite to that of a peptide strand, direct comparison to a peptide strand is difficult. Nevertheless, *β*-strand mimic **B** is equivalent in length to the main chain of a tetrapeptide (12 atoms) and may best be described as a tetrapeptide mimic.

Although *β*-sheets have a reputation for self-associating strongly and being insoluble, compounds containing *β*-strand mimic **B** are extremely tractable. Artificial *β*-sheet **2** has greater than 100 mM solubility in $CDCl_3$ and control **20** has greater than 25 mM solubility, and each of these compounds self-associates with dimerization constants of about 1 $M^{-1}$.[21] In contrast, Kemp's 2,8-diaminoepindolidione, which has hydrogen-bonding functionality along both edges, is only soluble in concentrated sulfuric acid.[2] Unlike a peptide strand, the other edge of *β*-strand mimic **B** is blocked by methoxy groups and offers no hydrogen-bonding functionality. The blockage of this edge may account for the low tendency of derivatives containing the *β*-strand mimic to self-associate and the high solubility of these compounds in organic solvents.[29]

*β*-Strand mimic **B** is readily prepared by the coupling of a 5-amino-2-methoxybenzoic acid unit with a 5-hydrazino-2-methoxybenzoic acid unit. *β*-Strand mimics of even greater length (e.g., **C** and **D**) might be prepared by combining the

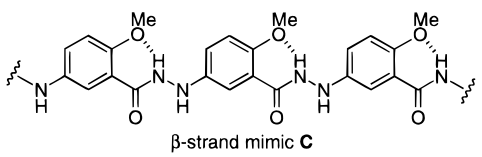


β-strand mimic **C**

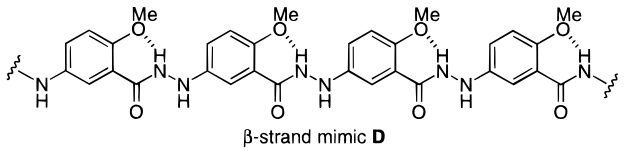


β-strand mimic **D**

5-amino-2-methoxybenzoic acid unit with two or more 5-hydrazino-2-methoxybenzoic acid units. In future studies, we will

(25) (a) Ribeiro, A. A.; Goodman, M.; Naider, F. *Int. J. Peptide Protein Research* **1979**, *14*, 414. (b) Stevens, E. S.; Sugawara, N.; Bonora, G. M.; Toniolo, C. *J. Am. Chem. Soc.* **1980**, *102*, 7048. (c) Gellman, S. H.; Adams, B. R. *Tetrahedron Lett.* **1989**, *30*, 3381.

(26) In competitive solvents, such as water and dimethyl sulfoxide, the chemical shifts of peptide amide protons exhibit different temperature dependencies: Solvent-exposed protons exhibit large temperature dependencies, while intramolecularly hydrogen-bonded (solvent-shielded) protons exhibit small temperature dependencies.

(27) (a) Kessler, H. *Angew. Chem., Int. Ed. Engl.* **1982**, *21*, 512. (b) Dyson, H. J.; Wright, P. E. *Annu. Rev. Biophys. Biophys. Chem.* **1991**, *20*, 519.

(28) Wüthrich, K. *NMR of Proteins and Nucleic Acids*; Wiley: New York, 1986; pp 166−168.

determine whether β-strand mimics such as these can be synthesized and whether they template β-sheet formation in peptide strands. We are particularly interested in learning whether the unprotected aniline-type amino groups will complicate coupling reactions during the preparation of higher oligomers and whether the twist about the hydrazide N-N bonds will interfere with the mimicry of extended β-strand structures. We will address these issues in subsequent papers.

## Experimental Section

**5-Bromo-2-methoxybenzoic Acid (5a).**[17] A mixture of bromine (5.6 mL, 109 mmol), 100 mL of dichloromethane, 100 mL of water, and *o*-anisic acid (15.2 g, 100 mmol) was stirred for 19 h. Excess bromine was destroyed by addition of $NaHSO_3$ (1.15 g, 11.0 mmol), the layers were separated, and the aqueous layer was extracted sequentially with a 100-mL and a 50-mL portion of methylene chloride. The combined organic layers were dried over $MgSO_4$, filtered, and concentrated by rotary evaporation. The resulting solid residue was suspended in 40 mL of dichloromethane and triturated with 500 mL of ice-cold hexanes. The suspension was filtered, and the precipitate was washed with ice-cold hexanes and dried to afford 22.1 g (96%) of acid **5a** as a white solid: mp 119−120 °C; IR ($CHCl_3$) 3307, 1738 $cm^{-1}$; $^1H$ NMR (300 MHz, $CDCl_3$) $\delta$ 8.27 (d, $J$ = 2.6 Hz, 1 H), 7.67 (dd, $J$ = 8.8, 2.6 Hz, 1 H), 6.97 (d, $J$ = 8.9 Hz, 1 H), 4.07 (s, 3 H); HRMS (EI) *m/e* for $C_8H_7BrO_3$ ($M^+$), calcd 229.9579, found 229.9576. Anal. Calcd for $C_8H_7BrO_3$: C, 41.59; H, 3.05. Found: C, 41.70; H, 2.89.

**Acid 6a.** A 250-mL, three-necked, round-bottomed flask equipped with a nitrogen inlet adapter, a glass stopper, a rubber septum, and a magnetic stirring bar was charged with ca. 100 mL of dry tetrahydrofuran, cooled to −78 °C, and charged with 27.5 mL of a 1.6 M solution of *n*-butyllithium in hexanes (44 mmol). 5-Bromo-2-methoxybenzoic acid (4.62 g, 20.0 mmol) was added in a single portion, and the reaction mixture was stirred for 15 min. Di-*tert*-butylazodicarboxylate (5.53 g, 24.0 mmol) was added in a single portion, the reaction mixture stirred for 5 min, and the cooling bath was removed. After 20 min, 100 mL of water was added, the layers were separated, and the aqueous phase was washed with 50 mL of ether. Ethyl acetate (100 mL) and 1 M aqueous HCl (44 mL) were added to the aqueous phase, the layers were separated, and the aqueous layer was extracted with 30 mL of ethyl acetate. The combined ethyl acetate layers were dried over $MgSO_4$, filtered, and concentrated by rotary evaporation to a viscous yellow oil. The residue was dissolved in ether and allowed to stand overnight. The resulting suspension was filtered, and the solid residue was washed with ether to afford 2.89 g (38%) of acid **6a** as a white solid: mp 174−175 °C dec; IR ($CHCl_3$) 3400, 3305, 1738 $cm^{-1}$; $^1H$ NMR (300 MHz, $CDCl_3$) $\delta$ 10.77 (br s, 1 H), 8.18 (br s, 1 H), 7.80 (br s, 0.7 H), 7.63 (br s, 0.3 H), 7.01 (d, $J$ = 9.0 Hz, 1 H), 6.82 (br s, 0.8 H), 6.64 (br s, 0.2 H), 4.07 (s, 3 H), 1.49 (s, 18 H); HRMS (FAB) *m/e* for $C_{18}H_{26}N_2O_7$ ($M^+$), calcd 382.1740, found 382.1747. Anal. Calcd for $C_{18}H_{26}N_2O_7$: C, 56.54; H, 6.85; N, 7.33. Found: C, 56.72; H, 6.74; N, 7.11.

**Amine 15.** A solution of $C_6H_5NH(CH_2)_2NH(CH_2)_2CN$[14b] (0.189 g, 1.00 mmol) and di-*tert*-butyl dicarbonate (0.218 g, 1.00 mmol) in 10 mL of dichloromethane was stirred for 2.3 h under $N_2$ and then concentrated by rotary evaporation. Column chromatography of the residue on silica gel (EtOAc−hexanes, 3:5) afforded 0.217 g (75%) of amine **15** as a colorless, viscous oil: IR ($CHCl_3$) 3444, 3429, 3402, 2252, 1689 $cm^{-1}$; $^1H$ NMR (500 MHz, $CDCl_3$) $\delta$ 7.18 (t, $J$ = 7.6 Hz, 2 H), 6.71 (br s, 1 H), 6.60 (d, $J$ = 7.0 Hz, 2 H), 4.16 (br s, 0.5 H), 3.91 (br s, 0.5 H), 3.53 (br s, 2 H), 3.48 (t, $J$ = 6.5 Hz, 2 H), 3.33 (appar. t, $J$ = 5.4 Hz, 2 H), 2.65 (br s, 1 H), 2.54 (br s, 1 H), 1.49 (s, 9 H); HRMS (FAB) *m/e* for $C_{16}H_{23}N_3O_2$ ($M^+$), calcd 289.1790, found 289.1796. Anal. Calcd for $C_{16}H_{23}N_3O_2$: C, 66.41; H, 8.01; N, 14.52. Found: C, 66.43; H, 7.86; N, 14.38.

**Urea 16.** Phenylalanylisoleucylleucine methyl ester hydrochloride (0.444 g, 1.00 mmol) was converted to phenylalanylisoleucylleucine methyl ester isocyanate as described in ref 19. A solution of the isocyanate and amine **15** (1.09 g, 3.76 mmol) in 2 mL of dichloromethane was stirred under nitrogen for 20 h and then concentrated by rotary evaporation. Column chromatography of the residue on silica gel (EtOAc−hexanes, 1:1) afforded 0.543 g (75%) of PhN(CO-Phe-Ile-Leu-OMe)$CH_2CH_2$N(Boc)$CH_2CH_2$CN as a colorless oil: IR ($CHCl_3$) 3425, 3325, 2252, 1741, 1687, 1674 $cm^{-1}$; $^1H$ NMR (500 MHz, $CDCl_3$) $\delta$ 7.34 (m, 3 H), 7.21 (br s, 3 H), 6.99 (m, 4 H), 6.80 (d, $J$ = 8.5 Hz, 1 H), 6.43 (d, $J$ = 7.4 Hz, 0.5 H), 6.35 (d, $J$ = 7.4 Hz, 0.5 H), 4.63−4.47 (m, 3 H), 4.26 (t, $J$ = 7.3 Hz, 1 H), 3.72 (s, 3 H), 3.83−3.62 (m, 2 H), 3.54−3.32 (m, 4 H), 3.04 (dd, $J$ = 14.1, 5.3 Hz, 1 H), 2.96−2.88 (m, 1 H), 2.64−2.54 (m, 2 H), 1.95−1.87 (m, 1 H), 1.70−1.60 (m, 2 H), 1.60−1.54 (m, 1 H), 1.42 (br s, 5 H), 1.25 (s, 5 H), 1.12-1.03 (m, 1 H), 0.94 (appar. t, $J$ = 5.3 Hz, 6 H), 0.89 (t, $J$ = 7.3 Hz, 3 H), 0.86 (d, $J$ = 6.8 Hz, 3 H); HRMS (FAB) *m/e* for $C_{39}H_{57}N_6O_7$ $(M + H)^+$, calcd 721.4288, found 721.4292. Anal. Calcd for $C_{39}H_{56}N_6O_7$: C, 64.98; H, 7.83; N, 11.66. Found: C, 64.80; H, 7.74; N, 11.52.

A solution of PhN(CO-Phe-Ile-Leu-OMe)$CH_2CH_2$N(Boc)$CH_2CH_2$-CN (0.252 g, 0.350 mmol) in 10 mL of a saturated solution of methylamine in methanol was allowed to react under nitrogen for 2 h and then concentrated by rotary evaporation to afford 0.255 g of a white solid. Column chromatography on silica gel (EtOAc) afforded 0.237 g (94%) of urea **16** as a foamy, white solid: IR ($CH_2Cl_2$) 3388, 3307, 2252, 1664, 1659 $cm^{-1}$; $^1H$ NMR (500 MHz, $CDCl_3$) $\delta$ 7.33 (br s, 4 H), 7.23−7.14 (m, 4 H), 7.01−7.03 (m, 1 H), 7.02−6.95 (m, 2 H), 6.95−6.88 (m, 2 H), 4.82−4.73 (m, 1 H), 4.62 (br s, 0.5 H), 4.54 (br s, 1 H), 4.48 (br s, 0.5 H), 4.38−4.29 (m, 1 H), 3.86−3.27 (m, 6 H), 3.11 (dd, $J$ = 13.9, $J$ = 4.6 Hz, 1 H), 2.80 (dd, $J$ = 13.6, $J$ = 8.1 Hz, 1 H), 2.73−2.47 (m, 5 H), 1.98−1.87 (br s, 1 H), 1.86−1.76 (m, 1 H), 1.65−1.53 (m, 2 H), 1.53−1.45 (m, 1 H), 1.42 (s, 4.5 H), 1.24 (s, 4.5 H), 1.04−1.16 (m, 1 H), 0.90 (m, 12 H); HRMS (FAB) *m/e* for $C_{39}H_{58}N_7O_6$ $(M + H)^+$, calcd 720.4448, found 720.4446.

**2-Methoxy-5-nitrobenzoic Acid.**[30] To an ice-cooled suspension of *o*-anisic acid (1.52 g, 10.0 mmol) in 20 mL of concentrated sulfuric acid was added $NH_4NO_3$ (0.890 g, 11.0 mmol) in small portions over 20 min. The ice bath was removed, and the reaction mixture was allowed to warm to room temperature over 20 min and then poured into 100 mL of water. The resulting suspension was filtered, and the precipitate was washed with 300 mL of water, dissolved in methanol, and reisolated by rotary evaporation to afford 1.49 g (75%) of 2-methoxy-5-nitrobenzoic acid as a white solid: mp 161−162 °C; IR ($CHCl_3$) 3358, 1745, 1346 $cm^{-1}$; $^1H$ NMR (300 MHz, $CDCl_3$) $\delta$ 9.00 (d, $J$ = 2.9 Hz, 1 H), 8.46 (dd, $J$ = 9.1, 2.9 Hz, 1 H), 7.19 (d, $J$ = 9.3 Hz, 1 H), 4.17 (s, 3 H); HRMS (CI, isobutane) *m/e* for $C_8H_8NO_5$ $(M + H)^+$, calcd 198.0402, found 198.0398. Anal. Calcd for $C_8H_7NO_5$: C, 48.74; H, 3.58; N, 7.10. Found: C, 48.64; H, 3.46; N, 7.00.

**Benzyl 2-Methoxy-5-nitrobenzoate.** A suspension of 2-methoxy-5-nitrobenzoic acid (1.01 g, 5.12 mmol) in 5.0 mL of thionyl chloride and 0.02 mL of *N*,*N*-dimethylformamide was heated at reflux for 2 h and then concentrated by rotary evaporation to afford 2-methoxy-5-nitrobenzoyl chloride as a yellow solid. A solution of benzyl alcohol (0.259 mL, 2.50 mmol), triethylamine (0.348 mL, 2.50 mmol), 4-(dimethylamino)pyridine (0.031 g, 0.25 mmol), and a portion of the crude acid chloride (0.457 g, 2.12 mmol) in 10 mL of dichloromethane was stirred under nitrogen for 20.5 h. Dichloromethane (10 mL) and 20 mL of water was added to the reaction mixture, and the aqueous phase was then acidified to pH 4 with 1 M aqueous HCl. The phases were separated, the aqueous phase was extracted with 5 mL of dichloromethane, and the combined organic layers were washed with 5 mL of saturated aqueous $NaHCO_3$. The aqueous layer was extracted with 5 mL of dichloromethane, and the combined organic layers were dried over $Na_2SO_4$, decanted, and concentrated by rotary evaporation. Column chromatography of the residue on silica gel (EtOAc−hexanes, 1:1) afforded 0.490 g (80%) of benzyl 2-methoxy-5-nitrobenzoate as a pale yellow solid: mp 95−96 °C; IR ($CHCl_3$) 1728, 1346 $cm^{-1}$; $^1H$ NMR (500 MHz, $CDCl_3$) $\delta$ 8.69 (d, $J$ = 2.8 Hz, 1 H), 8.33 (dd, $J$ = 9.3, 2.9 Hz, 1 H), 7.45 (d, $J$ = 7.4 Hz, 2 H), 7.39 (t, $J$ = 7.4 Hz, 2 H),

(29) (a) Rajarathnam, K.; Sykes, B. D.; Kay, C. M.; Dewald, B.; Geiser, T.; Baggiolini, M.; Clark-Lewis, I. *Science* **1994**, *264*, 90. (b) Ghadiri, M. R.; Kobayashi, K.; Granja, J. R.; Chadha, R. K.; McRee, D. E. *Angew. Chem., Int. Ed. Engl.* **1995**, *34*, 93. (c) Kobayashi, K.; Granja, J. R.; Ghadiri, M. R. *Angew. Chem., Int. Ed. Engl.* **1995**, *34*, 95. (d) Nesloney, C. L; Kelly, J. W. *J. Am. Chem. Soc.* **1996**, *118*, 5836.

(30) de Paulis, T.; Janowsky, A.; Kessler, R. M.; Clanton, J. A.; Smith, H. E. *J. Med. Chem.* **1988**, *31*, 2027.

7.34 (t, $J$ = 7.1 Hz, 1 H), 7.05 (d, $J$ = 9.3 Hz, 1 H), 5.36 (s, 2 H) 3.99 (s, 3 H); HRMS (EI) *m/e* for $C_{15}H_{13}NO_5$ ($M^+$), calcd 287.0794, found 287.0782. Anal. Calcd for $C_{15}H_{13}NO_5$: C, 62.72; H, 4.56; N, 4.88. Found: C, 62.60; H, 4.53; N, 4.92.

**Benzyl 5-Amino-2-methoxybenzoate.** A suspension of benzyl 2-methoxy-5-nitrobenzoate (0.179 g, 0.623 mmol) and stannous chloride dihydrate (0.703 g, 3.11 mmol) in 6 mL of ethyl acetate was heated at reflux for 19.5 h and then partitioned between 20 mL of ethyl acetate and 45 mL of half-saturated aqueous sodium bicarbonate. The aqueous layer was extracted with 20 mL of ethyl acetate, and the combined organic layers were washed with 5 mL of saturated aqueous NaCl, dried over $MgSO_4$, filtered, and concentrated by rotary evaporation to give 0.151 g of a yellow oil. Column chromatography on the residue on silica gel (EtOAc−hexanes, 1:1) afforded 0.115 g (72%) of benzyl 5-amino-2-methoxybenzoate as a pale yellow oil: IR ($CHCl_3$) 3444, 3369, 1718 $cm^{-1}$; $^1H$ NMR (300 MHz, $CDCl_3$) $\delta$ 7.38 (m, 5 H), 7.16 (s, 1 H), 6.80 (s, 2 H), 5.32 (s, 2 H), 3.81 (s, 3 H), 3.48 (s, 2 H); HRMS (CI) *m/e* for $C_{15}H_{16}NO_3$ ($M^+$), calcd 257.1052, found 257.1059. Anal. Calcd for $C_{15}H_{15}NO_3$: C, 70.02; H, 5.88; N, 5.44. Found: C, 70.30; H, 5.66; N, 5.28.

**Benzyl Ester 18.** A mixture of urea **16** (0.488 g, 0.678 mmol) and 7 mL of a ca. 2.5 M solution of HCl in methanol was allowed to react under nitrogen for 19 h and then concentrated by rotary evaporation. The residue was dissolved in 10 mL of water, and the solution was made basic (ca. pH 9) by addition of 6 M aqueous NaOH and extracted with three 10-mL portions of dichloromethane. The combined organic layers were dried over $MgSO_4$, filtered, and concentrated by rotary evaporation to afford 0.422 g of a foamy, white solid. Column chromatography on silica gel (MeOH−EtOAc, 1:20) afforded 0.343 g (82%) of PhN(CO-Phe-Ile-Leu-OMe)$CH_2CH_2NHCH_2CH_2CN$ as a foamy, white solid: mp 81−82 °C; IR ($CHCl_3$) 3419, 3385, 3305, 2251, 1657 $cm^{-1}$; $^1H$ NMR (500 MHz, $CDCl_3$) $\delta$ 7.42−7.35 (m, 4 H), 7.23 (t, $J$ = 7.3 Hz, 1 H), 7.18 (t, $J$ = 7.2 Hz, 2 H), 7.03 (s, 1 H), 7.02 (d, $J$ = 2.4 Hz, 1 H), 6.94 (appar. q, $J$ = 4.3 Hz, 1 H), 6.88 (d, $J$ = 7.2 Hz, 2 H), 6.79 (d, $J$ = 6.1 Hz, 1 H), 4.67 (appar. s, 1 H), 4.50 (ddd, $J$ = 10.9, 8.2, 3.8 Hz, 1 H), 4.29 (dt, $J$ = 8.4, 4.2 Hz, 1 H), 4.23 (dd, $J$ = 6.6, 4.4 Hz, 1 H), 3.76 (dt, $J$ = 14.1, 6.2 Hz, 1 H), 3.66 (dt, $J$ = 14.1, 6.0 Hz, 1 H), 3.13 (dd, $J$ = 14.0, 4.7 Hz, 1 H), 2.89−2.81 (m, 2 H), 2.79 (d, $J$ = 4.7 Hz, 3 H), 2.73 (dd, $J$ = 14.1, 9.1 Hz, 1 H), 2.69 (t, $J$ = 6.1 Hz, 2 H), 2.43 (t, $J$ = 6.4 Hz, 2 H), 2.09−2.01 (m, 1 H), 1.86 (ddd, $J$ = 14.0, 10.0, 4.0 Hz, 1 H), 1.70−1.58 (m, 2 H), 1.50−1.41 (m, 1 H), 1.17−1.07 (m, 1 H), 0.94 (d, $J$ = 7.2 Hz, 6 H), 0.91 (d, $J$ = 6.3 Hz, 3 H), 0.90 (t, $J$ = 7.4 Hz, 3 H); HRMS (FAB) *m/e* for $C_{34}H_{50}N_7O_4$ ($M + H$)$^+$, calcd 620.3924, found 620.3911. Anal. Calcd for $C_{34}H_{49}N_7O_4$: C, 65.89; H, 7.97; N, 15.82. Found: C, 65.64; H, 7.93; N, 15.66.

[CAUTION: PHOSGENE IS VOLATILE AND HIGHLY TOXIC—USE HOOD]. A 1.93 M solution of phosgene in toluene (0.56 mL, 1.1 mmol) was added to a rapidly stirred, ice-cooled solution of benzyl 5-amino-2-methoxybenzoate (0.166 g, 0.645 mmol) in 5 mL of methylene chloride and 5 mL of saturated aqueous $NaHCO_3$ solution. After 15 min, the phases were separated, the organic phase was extracted with two 5-mL portions of methylene chloride, and the combined organic phases were dried over $MgSO_4$, filtered, and concentrated by rotary evaporation. The residue was dissolved in 2 mL of methylene chloride, and a solution of PhN(CO-Phe-Ile-Leu-OMe)$CH_2CH_2NHCH_2$-$CH_2CN$ (0.333 g, 0.537 mmol) in 3 mL of dichloromethane was added. The mixture was allowed to react under nitrogen for 2 h and was then concentrated by rotary evaporation to afford a foamy, pale yellow solid. Column chromatography on silica gel (EtOAc−dichloromethane, 3:1) afforded 0.434 g (89%) of benzyl ester **18** as a white powder: mp 199−200 °C; IR ($CHCl_3$) 3412, 3307, 2251, 1711 (sh), 1660 $cm^{-1}$; $^1H$ NMR (500 MHz, $CDCl_3$) $\delta$ 9.07 (s, 1 H), 8.16 (d, $J$ = 2.6 Hz, 1 H), 7.91 (dd, $J$ = 9.0, 2.7 Hz, 1 H), 7.48 (d, $J$ = 7.4 Hz, 2 H), 7.41−7.35 (m, 5 H), 7.32 (t, $J$ = 7.4 Hz, 1 H), 7.22−7.18 (m, 3 H), 7.05−7.01 (m, 2 H), 6.99−6.93 (m, 4 H), 6.39 (appar. q, $J$ = 4.7 Hz, 1 H), 6.20 (d, $J$ = 8.4 Hz, 1 H), 5.40 (s, 2 H), 4.76 (d, $J$ = 7.0 Hz, 1 H), 4.57 (q, $J$ = 7.1 Hz, 1 H), 4.39 (td, $J$ = 8.6, 5.9 Hz, 1 H), 4.16 (t, $J$ = 6.7 Hz, 1 H), 3.88 (s, 3 H), 3.81−3.68 (m, 3 H), 3.61−3.54 (m, 2 H), 3.45−3.39 (m, 1 H), 2.97 (dd, ABX pattern, $J_{AB}$ = 14.0 Hz, $J_{AX}$ = 6.4 Hz, 1 H), 2.89 (dd, ABX pattern, $J_{AB}$ = 13.9 Hz, $J_{BX}$ = 7.8 Hz, 1 H), 2.77−2.70 (m, 1 H), 2.72 (d, $J$ = 4.7 Hz, 3 H), 2.62 (dt, $J$ = 17.1, 5.9 Hz, 1 H), 1.81−1.70 (m, 1 H), 1.66 (ddd, $J$ = 13.7, 8.1, 5.8 Hz, 1 H), 1.54−1.47 (m, 1 H), 1.41 (ddd, $J$ = 13.6, 9.4, 6.0 Hz, 1 H), 1.36−1.30 (m, 1 H), 1.03−0.95 (m, 1 H), 0.85 (d, $J$ = 6.6 Hz, 3 H), 0.82 (d, $J$ = 6.5 Hz, 3 H), 0.77 (d, $J$ = 6.8 Hz, 3 H), 0.74 (t, $J$ = 7.4 Hz, 3 H); HRMS (FAB) *m/e* for $C_{50}H_{63}N_8O_8$ ($M + H$)$^+$, calcd 903.4768, found 903.4768. Anal. Calcd for $C_{50}H_{62}N_8O_8$: C, 66.50; H, 6.92; N, 12.41. Found: C, 66.47; H, 6.60; N, 12.39.

***N*-Methyl-5-hydrazino-2-methoxybenzamide Hydrochloride (19).** A solution of acid **6a** (0.382 g, 1.00 mmol), 1-hydroxybenzotriazole hydrate (0.230 g, 1.50 mmol), and 1-ethyl-3-(3′-dimethylaminopropyl)-carbodiimide hydrochloride (0.230 g, 1.20 mmol) in 10 mL of methanol was allowed to react under nitrogen for 24 min, and 2 mL of a saturated solution of methylamine in methanol was then added. After 2 h, the mixture was concentrated by rotary evaporation, and the residue was partitioned between 20 mL of water and 20 mL of dichloromethane. The aqueous layer was extracted with two 5-mL portions of dichloromethane, and the combined organic layers were dried over $MgSO_4$, filtered, and concentrated by rotary evaporation to give 0.460 g of an orange solid. Column chromatography on silica gel (EtOAc−hexanes, 3:1) afforded 0.335 g (85%) of the methylamide derivative of acid **6a** as a white solid: mp 183−184 °C dec; IR ($CHCl_3$) 3421, 1741, 1714, 1651 $cm^{-1}$; $^1H$ NMR (300 MHz, $CDCl_3$) $\delta$ 8.23 (br s, 0.3 H), 8.19 (br s, 0.7 H), 7.84 (br s, 1 H), 7.66 (br s, 0.7 H), 7.47 (br s, 0.3 H), 6.88−7.01 (m, 1.7 H), 6.60 (br s, 0.3 H), 3.95(s, 3 H), 3.01(d, $J$ = 4.8 Hz, 3 H) and 1.48 (s, 18 H); HRMS (FAB) *m/e* for $C_{19}H_{30}N_3O_6$ ($M + H$)$^+$, calcd 396.2134, found 396.2146. Anal. Calcd for $C_{19}H_{29}N_3O_6$: C, 57.71; H, 7.39; N, 10.63. Found: C, 57.74; H, 7.18; N, 10.45.

A solution of the methylamide derivative of acid **6a** (0.190 g, 0.480 mmol) in 5 mL of a ca. 2.5 M solution of HCl in methanol was permitted to react for 26 h and was then concentrated by rotary evaporation to afford 0.122 g (110%) of *N*-methyl-5-hydrazino-2-methoxybenzamide hydrochloride (or dihydrochloride) as an orange solid: mp 154−156 °C dec; IR (Nujol mull) 3600−2500, 1641 $cm^{-1}$; $^1H$ NMR (300 MHz, $D_2O$) $\delta$ 7.46 (d, $J$ = 2.9 Hz, 1 H), 7.23 (dd, $J$ = 9.0, 2.9 Hz, 1 H), 7.13 (d, $J$ = 9.0 Hz, 1 H), 3.90 (s, 3 H) and 2.88 (s, 3 H); HRMS (CI) *m/e* for $C_9H_{12}N_3O_2$ ($M - HCl - H$)$^+$, calcd 194.0929, found 194.0923.

**Artificial $\beta$-Sheet 2.** A two-necked, 50-mL, round-bottomed flask equipped with a gas inlet adapter connected to a nitrogen/vacuum manifold, a gas inlet adapter fitted with a balloon filled with hydrogen, and a magnetic stirring bar was evacuated, filled with nitrogen, and then charged with 0.230 g of 10% Pd/C, 7.7 mL of tetrahydrofuran, and benzyl ester **18** (0.426 g, 0.472 mmol). The flask was evacuated, filled with hydrogen gas, and maintained under a hydrogen atmosphere for 14 h. The reaction mixture was then filtered through Celite, and the filtrate was concentrated by rotary evaporation to afford 0.383 g (100%) of the carboxylic acid derivative of **18** as a foamy, light yellow solid. This compound was used directly in the next step without further purification. HRMS (FAB) *m/e* for $C_{43}H_{57}N_8O_8$ ($M + H$)$^+$, calcd 813.4299, found 813.4306.

1-Ethyl-3-(3′-dimethylaminopropyl)carbodiimide hydrochloride (0.106 g, 0.552 mmol) was added to a solution of the product of the preceding reaction (0.359 g, 0.442 mmol), **19** (0.137 g, 0.590 mmol), triethylamine (0.092 mL, 0.66 mmol), and 1-hydroxybenzotriazole hydrate (0.075 g, 0.55 mmol) in 5 mL of methanol. The reaction mixture was stirred under nitrogen for 19 h and then concentrated by rotary evaporation. The residue was partitioned between 25 mL of water and 50 mL of dichloromethane, and the organic layer was extracted with 25 mL of saturated aqueous $NaHCO_3$, dried over $MgSO_4$, filtered, and concentrated by rotary evaporation. Column chromatography of the residue on silica gel (twice, first with *i*-PrOH−EtOAc−dichloromethane, 5:45:50, then with *i*-PrOH−EtOAc, 5:95) afforded 0.265 g (61%) of artificial $\beta$-sheet **2** as a pale yellow solid. Reverse-phase HPLC analysis on a $C_{18}$ column with an eluant of 70:30 $CH_3OH-H_2O$ and 254 nm UV detection indicated **2** to be 98.4% pure: mp 142−144 °C; IR ($CHCl_3$) 3410, 3305, 2251, 1651 $cm^{-1}$; $^1H$ NMR (500 MHz, $CDCl_3$) $\delta$ 9.94 (s, 1 H), 9.57 (d, $J$ = 5.9 Hz, 1 H), 8.65 (d, $J$ = 2.4 Hz, 1 H), 8.47 (d, $J$ = 5.8 Hz, 1 H), 8.39 (dd, $J$ = 8.9, 2.5 Hz, 1 H), 8.19−8.15 (m, 2 H), 8.12 (appar. q, $J$ = 4.7 Hz, 1 H), 8.08 (appar. q, $J$ = 4.4 Hz, 1 H), 7.38−7.29 (m, 3 H), 7.14−6.96 (m, 6 H), 6.94−6.88 (m, 3 H), 6.28 (d, $J$ = 7.0 Hz, 1 H), 5.00 (q, $J$ = 7.0 Hz, 1 H), 4.85 (d, $J$ = 8.5 Hz, 1 H), 4.41 (q, $J$ = 7.2 Hz, 1 H), 4.14 (t, $J$ = 9.1 Hz, 1 H), 4.11 (s, 3

H), 3.91 (s, 3 H), 3.86−3.78 (m, 1 H), 3.68−3.55 (m, 2 H), 3.54−3.40 (m, 3 H), 3.01 (d, $J$ = 4.7 Hz, 3 H), 2.88 (dd, ABX pattern, $J_{AB}$ = 14.1 Hz, $J_{AX}$ = 6.6 Hz, 1 H), 2.81 (d, $J$ = 4.4 Hz, 3 H), 2.78 (dd, ABX pattern, $J_{AB}$ = 14.0 Hz, $J_{BX}$ = 9.3 Hz, 1 H), 2.62−2.59 (m, 2 H), 1.67−1.53 (m, 3 H), 1.45 (ddd, $J$ = 12.6, 8.0, 5.9 Hz, 1 H), 1.42−1.33 (m, 1 H), 1.06−0.96 (m, 1 H), 0.93 (d, $J$ = 6.2 Hz, 3 H), 0.81 (d, $J$ = 6.5 Hz, 3 H), 0.79 (d, $J$ = 6.9 Hz, 3 H), 0.58 (t, $J$ = 7.3 Hz, 3 H); $^{13}$C NMR (125 MHz, $CDCl_3$) δ 172.9, 171.8, 170.8, 166.1, 165.1, 157.2, 155.5, 152.5, 151.6, 143.2, 140.9, 136.4, 134.7, 130.2, 129.0, 128.2, 128.0, 127.3, 126.5, 123.0, 122.3, 121.5, 119.3, 118.8, 118.5, 116.2, 112.1, 111.6, 57.6, 56.3, 55.6, 52.2, 50.5, 48.1, 45.1, 41.1, 38.1, 36.5, 26.4, 26.0, 24.63, 24.55, 22.49, 22.2, 17.4, 15.3, 10.6; HRMS (FAB) *m/e* for $C_{52}H_{68}N_{11}O_9$ $(M + H)^+$, calcd 990.5201, found 990.5191.

**Control 20.** [CAUTION: PHOSGENE IS VOLATILE AND HIGHLY TOXIC—USE HOOD]. A 1.93 M solution of phosgene in toluene (0.46 mL, 0.89 mmol) was added to a rapidly stirred ice-cooled solution of benzyl 5-amino-2-methoxybenzoate (0.115 g, 0.447 mmol) in 5 mL of methylene chloride and 5 mL of saturated aqueous $NaHCO_3$ solution. After 15 min, the phases were separated, and the aqueous phase was extracted with two 5-mL portions of methylene chloride. The combined organic phases were dried over $MgSO_4$, filtered, and concentrated by rotary evaporation. The residue was dissolved in 5 mL of methylene chloride, and diethylamine (0.092 mL, 0.89 mmol) was added. The mixture was allowed to react for 0.75 h and was then concentrated by rotary evaporation to give 0.160 g of a colorless oil. Column chromatography on silica gel (EtOAc−hexanes, 1:1) afforded 0.135 g (84%) of $5Et_2NCONH-2MeO-C_6H_3CO_2Bn$ as a colorless oil: IR ($CHCl_3$) 3462, 1720, 1657 cm$^{-1}$; $^1$H NMR (500 MHz, $CDCl_3$) δ 7.77 (dd, $J$ = 9.0, 2.8 Hz, 1 H), 7.59 (d, $J$ = 2.8 Hz, 1 H), 7.45 (d, $J$ = 7.3 Hz, 2 H), 7.38 (t, $J$ = 7.4 Hz, 2 H), 7.33 (t, $J$ = 7.2 Hz, 1 H), 6.93 (d, $J$ = 9.0 Hz, 1 H), 6.21 (s, 1 H), 5.34 (s, 2 H), 3.88 (s, 3 H), 3.35 (q, $J$ = 7.1 Hz, 4 H), 1.21 (t, $J$ = 7.1 Hz, 6 H); HRMS (CI) *m/e* for $C_{20}H_{25}N_2O_4$ ($M^+$), calcd 356.1736, found 356.1752. Anal. Calcd for $C_{20}H_{24}N_2O_4$: C, 67.40; H, 6.79; N, 7.86. Found: C, 67.09; H, 6.80; N, 7.80.

A two-necked, 50-mL, round-bottomed flask was equipped with a gas inlet adapter connected to a nitrogen/vacuum manifold, a gas inlet adapter was fitted with a balloon filled with hydrogen, and a magnetic stirring bar was evacuated, filled with nitrogen, and then charged with 0.070 g of 10% Pd/C, 4 mL of tetrahydrofuran, and $5Et_2NCONH-2MeO-C_6H_3CO_2Bn$ (0.137 g, 0.386 mmol). The flask was evacuated, filled with hydrogen gas, and maintained under a hydrogen atmosphere for 21 h. The reaction mixture was then filtered through Celite, and the filtrate was concentrated by rotary evaporation. The residue was dissolved in a mixture of 10 mL of water, 3 mL of saturated aqueous $NaHCO_3$, 1 mL of 1 M aqueous NaOH, and 20 mL of dichloromethane. The layers were separated, and the aqueous layer was acidified with 5 mL of 1 M aqueous HCl and extracted with two 8-mL portions of dichloromethane. The combined organic layers were dried over $Na_2SO_4$ and concentrated by rotary evaporation to afford 0.094 g (92%) of $5Et_2NCONH-2MeO-C_6H_3CO_2H$ as a foamy, white solid: mp 154−156 °C, IR ($CHCl_3$) 3462, 3379, 3290, 1732, 1657 cm$^{-1}$; $^1$H NMR (300 MHz, $CDCl_3$) δ 8.21 (d, $J$ = 7.6 Hz, 1 H), 7.93 (s, 1 H), 7.00 (m, 2 H), 4.05 (s, 3 H), 3.42 (q, $J$ = 7.1 Hz, 4 H), 1.23 (t, $J$ = 7.1 Hz, 6 H); HRMS (EI) *m/e* for $C_{13}H_{18}N_2O_4$ $(M)^+$, calcd 266.1266, found 266.1270. Anal. Calcd for $C_{13}H_{18}N_2O_4$: C, 58.64; H, 6.81; N, 10.52. Found: C, 58.37; H, 6.77; N, 10.22.

1-Ethyl-3-(3′-dimethylaminopropyl)carbodiimide hydrochloride (0.092 g, 0.480 mmol) was added to a solution of $5Et_2NCONH-2MeO-C_6H_3-CO_2H$ (0.082 g, 0.309 mmol), **19** (0.111 g, 0.480 mmol), triethylamine (0.074 mL, 0.53 mmol), and 1-hydroxybenzotriazole hydrate (0.065 g, 0.48 mmol) in 5 mL of methanol. The mixture was allowed to react under nitrogen for 4 h and was then concentrated by rotary evaporation. The residue was partitioned between 20 mL of water and 20 mL of dichloromethane. The aqueous phase was then acidified to pH 1 with 1 M aqueous HCl, and the layers were separated. The organic layer was extracted with 20 mL of saturated aqueous $NaHCO_3$, dried over $MgSO_4$, filtered, and concentrated by rotary evaporation. Column chromatography of the residue on silica gel (*i*-PrOH−$CHCl_3$, 1:9) afforded 0.112 g (82%) of urea **20** as an orange solid: Reverse-phase HPLC analysis on a $C_{18}$ column with an eluant of 50:50 $CH_3OH-H_2O$ and 254 nm UV detection indicated **21** to be 98.5% pure: mp 164−166 °C; IR ($CHCl_3$) 3460, 3410, 1657, 1651 cm$^{-1}$; $^1$H NMR (300 MHz, $CDCl_3$) δ 9.55 (d, $J$ = 4.3 Hz, 1 H), 8.02 (dd, $J$ = 9.0, 2.6 Hz, 1 H), 7.90 (appar. q, $J$ = 4.6 Hz, 1 H), 7.82 (d, $J$ = 2.7 Hz, 1 H), 7.70 (d, $J$ = 2.6 Hz, 1 H), 7.00 (dd, $J$ = 8.9, 2.8 Hz, 1 H), 6.96 (d, $J$ = 9.1 Hz, 1 H), 6.85 (d, $J$ = 8.8 Hz, 1 H), 6.55 (s, 2 H), 4.00 (s, 3 H), 3.88 (s, 3 H), 3.35 (q, $J$ = 7.1 Hz, 4 H), 2.97 (d, $J$ = 4.8 Hz, 3 H), 1.19 (t, $J$ = 7.1 Hz, 6 H); $^{13}$C NMR (125 MHz, $CDCl_3$) δ 165.8, 165.5, 154.8, 153.2, 152.3, 142.5, 133.5, 125.7, 123.0, 122.1, 119.5, 118.1, 117.7, 112.5, 112.2, 56.5, 56.3, 41.5, 26.5, 13.9; HRMS (CI) *m/e* for $C_{22}H_{30}N_5O_5$ $(M + H)^+$, calcd 444.2247, found 444.2238.

**Control 21.** A solution of PhN(Et)CO-Phe-Ile-Leu-OMe[19] (0.102 g, 0.184 mmol) in 15 mL of a saturated solution of methylamine in methanol was allowed to react under nitrogen for 1 h and then concentrated by rotary evaporation to afford 0.101 g of urea **21** as a tan film. Reverse-phase HPLC analysis on a $C_{18}$ column with an eluant of 80:20 $CH_3OH-H_2O$ and 254 nm UV detection indicated **21** to be 99.3% pure: mp 225−226 °C; IR ($CHCl_3$) 3421, 3388, 3300, 1669 (sh), 1655 cm$^{-1}$; $^1$H NMR (500 MHz, $CDCl_3$) δ 7.58 (d, $J$ = 8.1 Hz, 1 H), 7.42−7.35 (m, 3 H), 7.29−7.21 (m, 1 H), 7.18 (t, $J$ = 7.5 Hz, 2 H), 6.91−6.88 (m, 3 H), 6.84 (d, $J$ = 7.1 Hz, 2 H), 6.48 (d, $J$ = 6.4 Hz, 1 H), 4.53−4.48 (m, 2 H), 4.22 (dd, $J$ = 6.6 Hz, 3.5 Hz, 1 H), 4.16 (ddd, $J$ = 9.2, 4.2, 2.3 Hz, 1 H), 3.71−3.65 (m, 1 H), 3.59−3.54 (m, 1 H), 3.16 (dd, $J$ = 14.1, 4.4 Hz, 1 H), 2.82 (d, $J$ = 4.6 Hz, 3 H), 2.64 (dd, $J$ = 14.1, 9.7 Hz, 1 H), 2.17−2.10 (m, 1 H), 1.90 (ddd, $J$ = 13.9, 10.6, 3.6 Hz, 1 H), 1.73 (ddd, $J$ = 13.9, 11.9, 4.0 Hz, 1 H), 1.69−1.53 (m, 2 H), 1.52−1.44 (m, 1 H), 1.15−1.07 (m, 1 H), 1.03 (t, $J$ = 7.1 Hz, 3 H), 0.97−0.95 (m, 6 H), 0.92 (d, $J$ = 7.9 Hz, 3 H), 0.90 (d, $J$ = 7.2 Hz, 3 H); $^{13}$C NMR (125 MHz, $CDCl_3$) δ 173.3, 173.0, 170.6, 157.1, 139.7, 135.5, 130.5, 129.1, 128.5, 128.4, 128.0, 127.3, 59.1, 57.5, 52.0, 44.0, 39.6, 37.0, 35.5, 26.3, 25.0, 24.6, 23.4, 20.5, 16.2, 13.5, 11.7; HRMS (FAB) *m/e* calcd for $C_{31}H_{46}N_5O_4$ $(M + H)^+$, calcd 552.3550, found: 552.3554. Anal. Calcd for $C_{31}H_{45}N_5O_4$: C, 67.49; H, 8.22; N, 12.69. Found: C, 67.09; H, 8.29; N, 12.62.

**$^1$H NMR NOE Studies of Artificial β-Sheet 2.** A 25-mM solution of artificial β-sheet **2** in dry $CDCl_3$ was flame-sealed in an NMR tube after five freeze−pump−thaw cycles on a high-vacuum line. The 500 MHz $^1$H NMR spectra were recorded at 30 °C and 39 resonances were identified as follows: 1, δ 9.93 (s, 1 H); 2, δ 9.55 (s, 1 H); 3, δ 8.65 (d, $J$ = 2.8 Hz, 1 H); 4, δ 8.44 (br s, 1 H); 5, δ 8.39 (dd, $J$ = 9.0, 2.8 Hz, 1 H); 6, δ 8.15 (d, $J$ = 3.0 Hz, 1 H); 7, δ 8.14 (d, $J$ = 9.2 Hz, 1 H); 8, δ 8.10 (q, $J$ = 4.7 Hz, 1 H); 9, δ 8.01 (q, $J$ = 4.6 Hz, 1 H); 10, δ 7.37−7.30 (m, 3 H); 11, δ 7.10 (tt, $J$ = 7.1, 1.7 Hz, 1 H); 12, δ 7.08 (dd, $J$ = 8.8, 3.0 Hz, 1 H); 13, δ 7.05−6.99 (m, 4 H); 14, δ 6.98 (d, $J$ = 9.1 Hz, 1 H); 15, δ 6.91 (dd, $J$ = 8.0, 1.2 Hz, 2 H); 16, δ 6.90 (d, $J$ = 8.7 Hz, 1 H); 17, δ 6.17 (d, $J$ = 7.2 Hz, 1 H); 18, δ 5.00 (td, $J$ = 8.8, 6.8 Hz, 1 H); 19, δ 4.83 (d, $J$ = 8.5 Hz, 1 H); 20, δ 4.44 (q, $J$ = 7.3 Hz, 1 H); 21, δ 4.12 (t, $J$ = 9.0 Hz, 1 H); 22, δ 4.04 (s, 3 H); 23, δ 3.91 (s, 3 H); 24, δ 3.85−3.80 (m, 1 H); 25, δ 3.68−3.56 (m, 2 H); 26, δ 3.54−3.41 (m, 3 H); 27, δ 3.00 (d, $J$ = 4.8 Hz, 3 H); 28, δ 2.87 (dd, ABX pattern, $J_{AB}$ = 14.1 Hz, $J_{AX}$ = 6.6 Hz, 1 H); 29, δ 2.81 (d, $J$ = 4.7 Hz, 3 H); 30, δ 2.78 (dd, ABX pattern, $J_{AB}$ = 14.1 Hz, $J_{BX}$ = 9.3 Hz, 1 H); 31, δ 2.72−2.59 (m 2 H); 32, δ 1.67−1.54 (m, 3 H); 33, δ 1.45 (ddd, $J$ = 12.6, 8.0, 5.9 Hz, 1 H); 34, δ 1.42−1.34 (m, 1 H); 35, δ 1.06−0.95 (m, 1 H); 36, δ 0.93 (d, $J$ = 6.4 Hz, 3 H); 37, δ 0.81 (d, $J$ = 6.3 Hz, 3 H); 38, δ 0.79 (d, $J$ = 6.7 Hz, 3 H); 39, δ 0.59 (t, $J$ = 7.4 Hz, 3 H).

Twenty-two one-dimensional NOE experiments were performed with 3 s irradiation time and a collection of 512 transients. Percentage NOEs were calculated by comparing the area of the enhanced peak and are normalized to reflect the irradiation of multiple hydrogens but are not normalized to reflect enhancements of more than one proton. Enhanced peaks involving more than one proton are marked with an asterisk. Enhancements of 0.4% or greater are reported as follows: Irradiation of 1 enhanced 3 (4.4), 5 (0.7), 24 (1.5), 25 (4.1*), 26 (1.9*). Irradiation of 2 enhanced 6 (0.7), 12 (3.5), 22 (1.1*). Irradiation of 3 enhanced 1 (1.6), 18 (1.8). Irradiation of 4 enhanced 6 (2.1), 12 (0.9). Irradiation of 6 enhanced 18 (0.9, NOE attributed to nonselective irradiation in which 7 was also irradiated) 20 (1.1). Irradiation of 7 enhanced 3 (0.6), 18 (3.9), 21 (0.4), 32 (1.1), 34 (0.4). Irradiation of 8 enhanced 23 (0.8*), 27 (6.6*). Irradiation of 9 enhanced 6 (0.8), 20 (3.4), 27 (0.7*), 29 (6.9*), 32 (0.6). Irradiation of 17 enhanced 20 (1.1), 21 (3.3), 32 (2.4*), 33 (1.4). Irradiation of 18 enhanced 3 (2.2), 7 (3.4), 13 (5.4*),

28 (1.4), 30 (1.4). Irradiation of 19 enhanced 10 (0.4*), 13 (1.8*), 15 (2.5*). Irradiation of 20 enhanced 6 (2.3), 9 (3.1), 17 (0.5), 32 (1.8*), 33 (1.1), 36 (1.3*), 37 (1.8*). Irradiation of 21 enhanced 7 (0.9), 17 (1.8), 32 (1.5*), 34 (0.6), 35 (0.8), 38 (1.8*), 39 (0.9*). Irradiation of 22 enhanced 2 (0.6), 14 (6.4). Irradiation of 23 enhanced 8 (1.0), 16 (7.5). Irradiation of 27 enhanced 8 (5.6), 9 (0.4). Irradiation of 28 enhanced 13 (4.4*), 18 (3.1). Irradiation of 29 enhanced 9 (2.7). Irradiation of 36 enhanced 9 (0.6), 11 (0.5), 13 (1.3*), 20 (2.0), 27 (0.8*), 32 (6.0), 33 (1.9). Irradiation of 37 enhanced 20 (2.0), 32 (11.5), 33 (1.2). Irradiation of 38 enhanced 7 (0.7), 17 (0.4), 20 (0.4), 21 (2.6), 32 (4.1*), 34 (0.5), 35 (0.5), 39 (2.6*). Irradiation of 39 enhanced 21 (1.2), 32 (2.0), 34 (4.6), 35 (3.0).

**Acknowledgment.** This work was supported by the National Institutes of Health Grant GM-49076, Zeneca Pharmaceuticals Group, the Upjohn Company, and Hoffman-La Roche Inc. D.L.H. thanks the National Institute on Aging for support in the form of a training grant (National Research Service Award AG00096-12). J.S.N. thanks the following agencies for support in the form of awards: the Camille and Henry Dreyfus Foundation (New Faculty Award, Teacher-Scholar Award), the National Science Foundation (Young Investigator Award, Presidential Faculty Fellowship), and the Arnold and Mabel Beckman Foundation (Young Investigator Award).

**Supporting Information Available:** $^1$H NMR spectra and HPLC traces of compounds **2**, **20**, and **21**. Thermal ellipsoid plots, experimental details of the X-ray crystallographic structure determination, and tables of distances, angles, fractional coordinates, and thermal parameters for compounds **7a**, **7b**, and **9**−**13** (87 pages). See any current masthead page for ordering and Internet access instructions.

JA963843S